Spatial and temporal variation in hydrography, chlorophyll, and oxygen of San Juan Channel: effects of local and external factors

Kali Williams

Pelagic Ecosystem Function Apprenticeship
Fall 2012

Friday Harbor Laboratories, University of Washington, Friday Harbor, WA 98250

Contact Information:

Kali Williams

kalirwilliams@yahoo.com

School of Aquatics and Fishery Sciences

Keywords: Hydrography, Chlorophyll, Dissolved oxygen, Seasonal variation, Spatial variation, Interannual variation

Abstract

Situated between the Strait of Juan de Fuca and the Strait of Georgia, the San Juan Channel exists as a complex, dynamic, highly productive estuarine ecosystem—receiving oceanic input from the south and freshwater input from the north, respectively. Phytoplankton are highly important to marine ecosystems and studying the interactions between these organisms and the changing physical oceanographic environment is becoming increasingly important—especially in regions of high biological productivity such as the San Juan Channel. Stemming from the decided importance of these interactions, the purpose of this study was to build on our understanding of patterns and drivers of variation in the physical oceanography of the region—with a specific focus on oxygen and chlorophyll. We utilized measurements of temperature, salinity, density, chlorophyll fluorescence, and dissolved oxygen over the water column to assess variation both within fall 2012 and among fall data from 2004 to 2012. Correlations between density, chlorophyll, and oxygen were observed during fall 2012 and oceanic intrusions were seen as far as the north station—prior to the fall transition such intrusions were hypoxic and, presumably, had high CO_2 concentrations as well. An observed correlation proposed in 2011 and verified with these data between pycnocline variation and tidal height allows for the quantification of such intrusions. Comparison of the interannual data displayed unprecedentedly high levels of chlorophyll and dissolved oxygen, found during fall 2012. Analysis of the full data set revealed covariance of some variables, such as deep oxygen and temperature, as well as the influence of potential driving factors, such as tides, oceanic input, and Fraser River flow, on the pattern of interannual variation.

Introduction

Situated between the Strait of Juan de Fuca and the Strait of Georgia, the San Juan Channel exists as a complex, dynamic estuarine ecosystem—receiving oceanic input from the south and freshwater input from the north, respectively (Fig. 1). Estuaries are regions typically associated with high biological productivity and are therefore ecologically and economically valuable (Mann 1991). Water in the San Juan Channel is driven by estuarine circulation and tides, and interacts with local bathymetry, weather, seasonal shifts, coastal dynamics, and nearby water masses in a way that is conducive to supporting relatively high levels of biological productivity (McLaughlin 2009).

From approximately February to August northwesterly winds blow, paralleling the coastline and the California current (the waters of which the San Juan Channel is connected to via the Strait of Juan de Fuca); as the winds blow southward, Ekman transport pulls water offshore and dense, cold, nutrient-rich water is drawn up to take its place—a process commonly referred to as upwelling (Fig. 2) (Kudela 2008). Furthermore, the Fraser River—which delivers fresh water into the surface waters of the Strait of Georgia—has the highest amount of discharge during these months (Fig. 3) (Water 2012). This influx of fresh water, increased stratification, and the abundant sunlight characteristic of spring and summer lead to high biological productivity during these months.

Fall in the Pacific Northwest is a major transitional period. Typically beginning in September or October and continuing until spring, southeasterly winds prevail, Fraser River discharge decreases, and radiation decreases (Fig. 3). The shift from upwelling to downwelling (induced by the shift in wind direction from northwesterly to southeasterly) is known as the fall transition and brings warmer, fresher surface oceanic water, driven by Ekman transport, into the

system (Fig. 4) (Thomas 2011). All of these factors, as well as local processes, have important physical and biological implications for the region.

In order to understand and study a complex ecosystem such as the San Juan Channel, it is important to assess the physical context that organisms exist within. Specific oceanographic properties of the water column can be utilized to assess water origin, temporal and spatial patterns, as well as the physical and biological processes taking place at a given time. Hydrographic measurements of temperature and salinity (and from this density) in the San Juan Channel are important because they are useful in determining the origins of water masses present and can be used to characterize spatial and temporal patterns in the region of focus (Thomas 2011). Past research has shown that the density and movement of water in the channel affect the distribution of organisms and what nutrients and elements they have access to—especially small organisms such as phytoplankton and zooplankton (Mann 1991).

Phytoplankton are important because they play a major biological role in the environment by contributing to 95% of marine primary production, thus forming the base of the food web (Daly and Smith 1993). Considering the biological importance of phytoplankton in marine ecosystems, studying the interactions between these organisms and the changing physical oceanographic environment becomes increasingly more important—especially in regions of high biological productivity such as the San Juan Channel. Chlorophyll pigments in phytoplankton cells are essential to photosynthesis, and therefore essential to primary productivity and oxygen production (Denny 2008); accordingly, past research has demonstrated that chlorophyll is an effective predictor of phytoplankton abundance and distribution in this region (Meyer 2011). Understanding how these organisms are affected by the physical and chemical oceanography of the region is important, but it is also important to assess how these organisms affect the physical

and chemical oceanography—dissolved oxygen concentrations are an example of this interaction. It has been observed that biological processes are most typically responsible for the wide range of values of oxygen encountered. For example, through photosynthesis, phytoplankton growth can cause oxygen supersaturations, while respiratory processes can effectively remove all of the oxygen originally present in some water masses (Codispoti 1988). When compared to physical properties, evidence of these biological processes is apparent in the water column and these relationships can be monitored spatially and temporally. Continued studies of these interactions in the region will enable researchers to begin quantifying the effects that hydrography and biology exert on one another.

Stemming from the decided importance of these interactions, the purpose of this study was to build on our understanding of patterns and drivers of variation in the physical oceanography of the region—with a specific focus on oxygen and chlorophyll. Specific objectives were to 1) assess spatial and temporal variation in hydrography, chlorophyll, and oxygen, 2) determine which local and external factors affected oceanographic patterns this fall, and 3) compare 2012 to previous years (2004-2011).

Methods

Study Site

This study was conducted in the San Juan Channel in Washington State, USA at two specific sites that have been known to exhibit temporal and spatial variation: the North Station (48˚35.00’ N 123˚02.50’ W) and South Station (48˚25.20’ N, 122˚56.60’ W)(Fig. 1). Seven R/V Centennial cruises throughout September, October, and November collected data at the North and South station on an established North-South transect in the San Juan Channel (Table 1).

Data Collection

A Seabird SEACAT SBE-19 conductivity-temperature-depth instrument (CTD) was used to measure fluorescence (chlorophyll indicator), dissolved oxygen, temperature, and salinity at each station on each cruise date. For each CTD cast, the CTD sensor arrays were soaked at 10 meters for 3 minutes, zeroed at the surface, and then deployed to a depth approximately 10 meters from the seabed. During the descent and ascent of the CTD, real-time measurements of fluorescence, oxygen, temperature, and salinity were averaged over 0.5 meter bins and transmitted through a conducting cable to onboard computing systems (McLaughlin 2009). CTD sensor data were converted into Microsoft Excel spreadsheets using SBE Data Processing Software following the standard operating procedure generated by the JEMS lab (JEMS 1999).

During the ascent of the CTD, water samples were collected in 2-liter Niskin bottles at deployment depth (approximately 10 meters from the seabed), 50 meters, 30 meters, 10 meters, and at the surface. At each depth, 2 Niskin bottles were close via onboard computing systems. Onboard, water samples were extracted from the Niskins for discrete chlorophyll and oxygen analyses. Dissolved oxygen water samples were transferred from Niskins into calibrated 125mL Erlenmeyer flasks with fitted glass caps through VXR brand plastic tubing. Specific precautions were taken to avoid the addition of oxygen to the samples: VXR plastic tubing was squeezed from base to tip with water running through it to eliminate bubbles and flasks were flushed three times to eliminate any additional bubbles present. In accordance with the Carpenter modification of the Winkler titration method, 1 mL of MnCl2 and 1 mL of NaOH-NaI were added to fix the dissolved oxygen in the water samples and the bottles were inverted several times before placing in the box (Carpenter 1965). For chlorophyll water samples, opaque 0.065L bottles were rinsed three times, filled with water, and put in a cooler (Lorenzen 1986).

Hydrographic Analysis

CTD sensor temperature and salinity (and density) data were plotted versus depth on graphs in Microsoft Excel for each cruise date during Fall 2012.

Chlorophyll a and Phaeopigment Analysis: Fluorometric Method

In accordance with standard operating procedures (Newton et al 2002), chlorophyll water samples were filtered using Whatman GF/F (nominally 0.7 μm) glass microfiber filters coated with aqueous magnesium carbonate on a vacuum filtration rack. Filters were placed in plastic tubes and 10mL of 90% acetone (with distilled water) added, taking care to make sure the filter was fully immersed in the acetone. Samples were covered with aluminum foil and frozen until processing, extra care was taken to ensure that samples were not exposed to heat or light during this time. Acetone extracts were analyzed using a Turner 10 Analog fluorometer and readings were used to calculate chlorophyll and phaeopigment concentrations (Lorenzen, 1966). Fluorometer readings and CTD sensor fluorescence readings plotted against each other for each depth and linear regressions were run in order to determine a calibration equation to obtain calibrated fluorescence (chlorophyll indicator) values. Calibrated and uncalibrated CTD chlorophyll data were plotted versus depth in Microsoft Excel.

Dissolved Oxygen Analysis: Carpenter modification of Winkler Method

Dissolved oxygen water samples were sampled and processed based on the Carpenter modification of the Winkler titration Method (Carpenter 1965). At least 15 minutes after the addition of the chemicals, bottles were inverted several times to ensure the reaction was complete. Onshore, 1mL of H2SO4 was added to each solution and bottles were titrated to one thousandth of a milliliter with a sodium thiosulfate solution using a Beckman® 665 Dosimat microburet. Readings were used to calculate dissolved oxygen concentrations in the samples. The Winkler dissolved oxygen data were then plotted against the CTD oxygen sensor data for

each depth in order to determine a calibration equation to obtain calibrated dissolved oxygen values. Calibrated and uncalibrated CTD dissolved oxygen data were plotted versus depth in Microsoft Excel.

Tidal effects on vertical profiles of temperature, salinity, and oxygen

Based on parameters established by Katie Thomas in 2011, pycnocline variation at the south station was measured using variation in pycnocline width and depth and values were plotted versus tidal height in order to run linear regressions and determine correlation values (Thomas 2011). Pycnocline width was defined as the shallowest and deepest points at which there was a change in density > 0.02 Kg/m^3 for ≥ 3 consecutive 0.5m depth bins. Pycnocline depth was defined as the midpoint between the upper and lower limits of pycnocline width (Fig. 7). Tidal height data (MLLW) were acquired from the NOAA Tides and Currents webpage and plotted in Microsoft Excel for each cruise date in fall 2012 (Tide 2012). Only heights corresponding to south station sampling dates and times were used in this study (Table 2).

Interannual variation

Historical data for temperature, fluorescence (uncalibrated), and dissolved oxygen (uncalibrated and calibrated) were averaged for the north and south stations on each cruise date in each year (2004-2012) and plotted on graphs using Microsoft Excel; however, due to the variability of the data collection, only cruise dates that contained CTD drops for both stations and data for all of the variables of focus were used in comparisons. Interannual comparisons were made based on variation of the three variables in surface water (0m – 20 m) and deep water (60 m - 80 m or the bottom [whichever came first]).

Results

1: Fall 2012 hydrography, chlorophyll, and dissolved oxygen

1.1 Hydrography: temperature and salinity

CTD temperature and salinity sensor data displayed similar tends, of varying intensities, in the north and south stations from September 28th through November 14th:

a. North Station

The north station surface waters (approximately 0-20 m) got colder as the season progressed, with an approximate range of 10.63°C to 9.13° C, whereas the deep waters (approximately 70 m to 10 m above the seafloor) got warmer, ranging from approximately 8.95°C to 9.44°C (Fig. 9). Surface water salinity increased (with an approximate range of 29.24 PSU - 30.58 PSU) and deep-water salinity decreased as the season progressed (with an approximate range of 31.78 PSU – 30.39 PSU) (Fig. 10). On 10/10/2012, an intrusion of cold, salty, dense water was seen at depth.

b. South Station

The south station surface waters got colder as the season progressed, ranging from approximately 10.45°C to 9.07° C. Conversely, waters at depth got warmer and ranged from approximately 7.64°C to 8.99°C (Fig. 11). Salinity in the surface waters increased (with an approximate range of 29.94 PSU – 31.28 PSU) and deep-water salinity decreased (with an approximate range of 33.39 PSU – 31.88 PSU)(Fig. 12).

Temperature and salinity became more mixed at both stations as the season progressed—the north station was consistently more mixed than the south station. The south station was generally more stratified (Fig. 11-12) with highly variable pycnoclines (thermoclines and haloclines)(Fig. 8).

1.2 Chlorophyll

North station chlorophyll concentrations decreased in the surface waters (with an approximate range of 12.8 μg/L-0.43 μg/L) and stayed consistently low in deep water with no apparent seasonal or tidal trend (with an approximate range of 0.36 μg/L-1.14 μg/L)(Fig. 13). South station surface waters also showed a temporal decrease in chlorophyll concentrations (6.38 μg/L-1.02 μg/L) and consistently low levels at depth (0.33 μg/L-0.77 μg/L)(Fig. 14). The north station had higher maximum chlorophyll concentrations than the south station at the surface, but chlorophyll concentrations became uniformly low at both stations as the season progressed.

1.3 Dissolved oxygen

Dissolved oxygen concentrations decreased in the north station surface waters (with an approximate range of 7.93 mg/L - 5.64 mg/L) and increased at depth as the season progressed (with an approximate range of 4.48 mg/L – 6.46 mg/L)(Fig. 15). The surface water at south station also showed a temporal decrease in dissolved oxygen (7.22 mg/L – 5.85 mg/L) and increased levels at depth as the season progressed (3.02 mg/L – 5.51 mg/L)(Fig. 16). Dissolved oxygen concentrations became more mixed at both stations. The cold, saline intrusion of water seen in the deep water of the north station on 10/10/2012 also had the lowest oxygen concentrations seen at north station for fall 2012.

1.4 Hydrography versus Chlorophyll

Using density as an indicator of both temperature and salinity, linear regressions of chlorophyll versus density demonstrated that there is a moderate correlation between the two at both stations; typically, as density increases, chlorophyll decreases. North station R^2 values ranged from 0.00091 to 0.75637. South station R^2 values ranged from 0.1678 to 0.84305 (Table 3).

1.5 Chlorophyll versus dissolved oxygen

Linear regressions plotting chlorophyll versus dissolved oxygen for both stations demonstrated that a moderate correlation exists between the two measures; typically, as chlorophyll fluorescence increases, dissolved oxygen increases. North station R^2 values ranged from 0.01444 to 0.84824. South station R^2 values ranged from 0.19217 to 0.89981. Approximately 71% of the linear regressions (one for each station on each cruise date) had $R^2 > 0.3$ (Table 4).

1.6 Density versus dissolved oxygen

Linear regressions plotting density versus dissolved oxygen demonstrated that a strong correlation exists between the two for both stations—a stronger correlation than what was seen between chlorophyll and dissolved oxygen or between chlorophyll and density. Typically, as density increases dissolved oxygen concentrations decrease. North station R^2 values ranged from 0.22269 to 0.97558; the south station had consistently higher R^2 values that ranged from 0.91819 to 0.9909 (Table 5).

2: Tidal effects on vertical profiles of temperature, salinity, and dissolved oxygen

During a flood tide on October 10, 2012, prior to the fall transition (Fig. 6), intrusions of cold, salty, hypoxic water were seen in the deep waters of both stations—with stronger signals at the south station. As the season progressed, this pattern became less prominent in vertical profiles of temperature, salinity, and dissolved oxygen for both stations; rather, temperature and salinity at depth were consistently warmer and fresher, while dissolved oxygen concentrations were highly variable—but generally trended towards increasing levels at depth. Linear regressions plotting tidal height versus pycnocline width and depth displayed

weak correlations between the two for fall 2012 (R^2=0.48327 and R^2=0.02601, respectively) (Fig. 17-18).

3: Interannual comparison of temperature, chlorophyll, and dissolved oxygen

3.1 Temperature

Based on the multivariate ENSO index displayed and assessed by NOAA, 2012 was a weak to neutral El Niño year (Multivariate 2012). Relative to past neutral years (2004-2011), 2012 average surface temperatures (approximately 0-20 m) were comparable and followed similar patterns of decline as the season progressed at both stations—aside from a notable drop in temperature from October 17th through October 30th that brought average temperatures below the averages of previous La Niña years (Fig. 19-20). Average temperatures at depth (approximately 60-80 m) followed this same trend for the north station (Fig. 21); however, the south station temperatures at depth displayed this decline only on October 10th, after which temperatures rose back to levels comparable to previous neutral years (Fig. 22). Typically, on all of the plots, El Niño years have the highest average temperatures, La Niña years have the lowest average temperatures, and neutral years vary in and around those values.

3.2 Chlorophyll

The north station had unprecedentedly high levels of chlorophyll fluorescence during the first two cruises (ranging from approximately 4.14 µg/L to 10.89 µg/L)—whereas historically, averages ranged from approximately 0.93 µg/L to 4.01 µg/L during this time (Fig. 23). Chlorophyll levels at the south station were also markedly high for the first two cruises of fall 2012, with averages ranging from approximately 2.96 µg/L to 5.26 µg/L (historically, average surface fluorescence during this time has ranged between approximately 1.42 µg/L and 2.09 µg/L for the south station) (Fig 24).

3.3 Dissolved oxygen

Surface (0-20m) dissolved oxygen concentrations at both stations were higher than average for the first two cruise dates of 2012, and fell to moderate or average levels for the remainder of the cruises (Fig. 25-26). At depth (60-80m), oxygen concentrations stayed moderate and followed historical trends (Fig. 27-28). Surface oxygen concentrations tended to mimic surface fluorescence values, while oxygen levels at depth typically tended to mimic temperatures at depth.

Discussion:

Hydrographic patterns assessed and described by past Pelagic Ecosystem Function oceanographers, associated with external and local factors, were confirmed to be consistent with observations of fall 2012. This is especially true for the difference between water properties at the South versus North stations.

South station hydrography

On a local scale, it has been shown that decreases in atmospheric temperatures during the fall and winter months typically lead to associated decreases in surface water temperature—which was, in fact, observed at both stations during fall 2012. Past research has also shown that the San Juan Channel and surrounding regions exhibit changes associated with the shift from upwelling to downwelling known as the fall transition. Water entering the channel during flood tides and getting mixed into the channel prior to the fall transition is typically cold, salty, and nutrient-rich, as it originates from deep oceanic waters; however, the shift from upwelling to downwelling (induced by a shift in wind direction) mixes warmer, fresher oceanic water into the system (McLaughlin 2009). Oceanic water floods into the channel from the south via the Strait of Juan de Fuca; consequentially, the signature of oceanic input was consistently more

pronounced in the deep waters of the south station—consistent with observations from previous years (Fig. 11-12). This external influence accounts for the increase in temperature and decreases in salinity observed at depth in both stations beginning on 10/17/2012 (after the approximate fall transition observed in local upwelling indices; Fig. 6).

North station hydrography

The north station exhibited similar seasonal trends in temperature and salinity: surface waters cooled (local weather) and deep waters got warmer and fresher (from downwelled surface oceanic water)(Fig. 9-10). However, while the effects of upwelling and downwelling were more pronounced at the south station, the signature of the Fraser River plume was, as it has been shown to be in the past, more pronounced at the north station (Fig. 9-10). Fraser River discharge typically increases during the summer months due to increased runoff (Environment Canada, 2012), and with northerly winds the signature of this plume is often seen in the surface waters of the San Juan Channel. With the seasonal transition into fall, discharge decreases (Fig. 3) and the winds become predominantly southerly; past research has shown that these changes typically result in less fresh water influence in the surface waters of the channel (predominantly seen in the north station). Occasionally, however, fresh water signatures are seen later in the season, and 2012 displayed this trend on cruises three, four, and five (Fig. 10).

Studying hydrographic features such as temperature and salinity, and subsequently density, are important in determining the origin of water masses present (oceanic water from the Strait of Juan de Fuca and fresh water from the Fraser River via the Strait of Georgia, for example); however, assessments of these qualities can and should be extended beyond simple characterization of water masses present. Monitoring temperature and salinity on a temporal and spatial scale (seasonally, interannually, throughout the water column, and between stations)

enables researchers to establish typical patterns of variation in the region, discern atypical processes, and, ideally, begin extending this knowledge to the upper levels of the ecosystem—in order to continue developing knowledge of the physical-biological interface and assessing how organisms will be affected by such variation.

Chlorophyll-oxygen dynamics

Assessments of variation in chlorophyll and oxygen—the primary focus of this study—helped to determine how local and external physical processes affect the biology of the region at a very basic level. Phytoplankton abundance and distribution, as indicated by varying chlorophyll concentrations, are highly dependent on the stability of the water column and access to both nutrients (typically at depth) and photosynthetically active radiation (PAR) (from the surface) (Denny 2008). This relationship was reflected in the fall 2012 data (Fig. 13-14). During the first two cruises when PAR was higher and the water column was more stratified, phytoplankton were contained in the upper layers of the water column where they had access to the increased PAR. It is important to note that water samples taken to assess nutrient concentrations demonstrated that levels were more than sufficient for all cruise dates in fall 2012. Thus, with replete nutrients, sunlight and the water column stability needed in order to access the light were the factors driving phytoplankton abundance. After the Fall Transition, decreased PAR and the increased mixing typical of both stations during this time were associated with consistently low levels of chlorophyll fluorescence throughout the column, indicating that access to light was insufficient to support a larger phytoplankton population.

Chlorophyll distribution and concentrations are indicative of biological processes that commonly occur in the upper levels of the water column; however, assessments of oxygen

concentrations give insight into biological production (photosynthesis) and consumption (respiration), as well as physical processes, taking place throughout the water column.

Variability in oxygen concentrations have been shown to be both physically and biologically modulated in the past (McLaughlin 2009; Meyer 2011). Different densities of water (water masses) can support different types of organisms—considering the properties, nutrients, and processes typically associated with different densities of water, and different types of organisms exert different effects on the water column with respect to O_2 levels. Oxygen-producing organisms are typically found in the upper levels of the water column where they can utilize sunlight and nutrients to photosynthesize, oxygen-consuming organisms respire ubiquitously throughout the water column, and different water densities have variable holding capacities for oxygen because of the effect of both temperature and salinity on the solubility of dissolved oxygen in seawater (Denny 2008) (Fig. 5). While dissolved oxygen concentrations are determined by the interaction of these factors, the converse is also true that many organisms can only exist where oxygen concentrations are sufficient or of specific levels—the distribution of most heterotrophic organisms is determined by the availability of oxygen.

Strong correlations between density and both chlorophyll and oxygen were displayed throughout the season—with the strongest correlations existing between oxygen and density. Chlorophyll levels decreased as PAR decreased and both stations became more mixed; oxygen concentrations were found to be physically and biologically modulated as water masses changed and organisms within produced and consumed oxygen. This fall, dissolved oxygen displayed moderate correlations with chlorophyll fluorescence, which can be attributed to the production of oxygen during photosynthesis. However, vertical profiles of chlorophyll fluorescence and dissolved oxygen displayed differing trends at depth; changes in oxygen at depth can be

attributed to changes in water mass or respiration—but is typically a combination of the two. As density can account for the wide range of biological processes involved in the production and consumption of oxygen throughout the water column, rather than just at the surface, correlations between dissolved oxygen and density were consistently much stronger than those between oxygen and chlorophyll (Tables 4-5).

Oceanic intrusion into San Juan Channel

Patterns of variation associated with the Fall Transition, Fraser River discharge, and seasonal changes in weather have been assessed and characterized in previous years (i.e. McLaughlin 2009 and Meyer 2011). However, the appearance of cold, saline water seen at depth in the north station on 10/10/2012 appears to be linked to tidal forcing. An understanding of tidal influence on the water properties of the region, an important factor associated with variation throughout the channel, has only more recently emerged and offers an explanation for this phenomenon. The flooding tide on 10/10/2012 brought cold, saline, upwelled oceanic water into the channel from the south via the Strait of Juan de Fuca. Presumably, the much denser waters visible at depth in the north station were the signature of oceanic water flooding into the channel on that day. Thomas (2011) similarly found cold, saline, hypoxic water at depth in the north station during flood tides in fall 2011. While this trend became less discernable as the season progressed, this does not necessarily mean that transport northwards of waters from outside of the San Juan Channel on flooding tides stops; rather, with the shift from upwelling to downwelling, the oceanic surface water flooding into the channel was of a more similar composition to the water already present in the channel, and, therefore, the intrusions were less detectable, based on water properties (Fig. 9-12).

When considering the effects of such oceanic intrusions in the region, it is important to note that low levels of oxygen in dense waters are typically attributable to the consumption of oxygen that occurs during respiration (Denny 2008). Where respiration is occurring CO_2 is being produced (Fig. 5). Therefore, when dense, hypoxic oceanic water floods into the channel, presumably, this water will also be high in CO_2.

The observation that oceanic water flooding into the channel appears to be making it as far as the north station means that it will become increasingly important to quantify the magnitude and temporal variation of such intrusions—which building on Thomas's (2011) research offers promise. Her finding that pycnocline variation (Fig. 8) is tidally modulated offers the potential to quantify how thick the layer of water flooding into the channel is and thus may enable future researchers to begin assessing how such intrusions will affect the region and organisms present. Although the correlation between pycnocline variation and tidal height was not particularly strong for fall 2012, these data add to the correlation Thomas (2011) presented. Thomas's (2011) correlation was based on data from the full annual cycle of 2011 and, therefore, had a wider range of tidal heights with which to establish such correlations; whereas the range of tidal heights for fall 2012 cruise dates was relatively narrow. However, my findings do support the correlations and continuing to assess these correlations with more annual data will help define the consistency of this relationship.

Interannual patterns 2004-2012

The result that interannual dissolved oxygen concentrations follow fluctuations in fluorescence at the surface, while resembling temperature at depth, reveals the complexity of potential driving factors involved. There were unprecedentedly high levels of surface oxygen and fluorescence at both stations during the first two cruise dates in 2012, suggesting that the warm

air temperature and sunlight of fall 2012 had a positive effect on phytoplankton abundance. Despite local press noting that 2012 had an unusually prolonged summer, this did not translate to warmer water temperatures. In 2012, during cruises three, four and five, the coldest waters on record in this dataset were observed at both stations (Fig. 19-21). Future analysis of interannual patterns would benefit from comparing the dataset to the Pacific Decadal Oscillation (PDO) index as well as including salinity in comparisons.

In conclusion, perhaps the most notable finding of the study was the additional evidence that flooding tides are bringing oceanic water as far as the north station. As aforementioned, during the upwelling season, this oceanic water is not only hypoxic, but also naturally high in CO_2 due to respiration. In light of global ocean acidification, the naturally high levels of CO_2 flooding into the San Juan Channel would produce an additive effect that makes this region, and similar regions, more susceptible to the effects of CO_2. This means that it will become increasingly more important to find ways to quantify the spatial and temporal footprint of these effects—and the emerging correlation between tides and such oceanic intrusions is an encouraging first step.

Acknowledgements

This work could not have been completed with out Jan Newton who taught data collection methods and provided invaluable guidance and support throughout this study. Ryan McLaughlin was indispensable in data analyses and was always cheerful and willing to help. Breck Tyler and Matt Baker were also crucial components of the teaching team and taught data collection and gave necessary feedback. My fellow apprentices Gina Contolini, Todd Sigley, Gavin Brackett, Nick Sisson, Charlie Heller, Annie Thomson, Jessica Nordstrom, Grace Teller, Bryson Albrecht,

and Morgan Einslord not only helped with data collection and analyses, but supported me academically and emotionally and helped make this a great experience. Finally, Dennis Willows, Wolf Kreiger, Phil Green, Gary Greene, Loren Tuttle, Julie Keister, Craig Staude, Alan Cairns, David Duggins, Jeannie Meredith, Kristy Kull, Pema Kitaeff, Maureen Nolan, Henry and Holly Wendt, Stacy Markman, the entire FHL staff, University of Washington Provost, and the Mary Gates Endowment who provided additional indispensable, vastly appreciated, support and guidance during this study.

References:

Carpenter, J. H. 1965. The accuracy of the Winkler method for dissolved oxygen. *Limnology and Oceanography,10*, 135-140.

Codispoti, Lou. 1988. One Man's Advice on the Determination of Dissolved Oxygen in Seawater. *University of Washington*. <http://courses.washington.edu/ocean220/misc/OxygenProtocol.pdf>. 1-11.

Daly, K. L. and Smith, W. O. 1993. Physical-biological interactions influencing marine plankton production. *Annual review of Ecological Systems,24*: 555-585.

Denny, M. (2008). How the ocean works: an introduction to oceanography. Princeton University Press: 61-230.

Joint Effort to Monitor the Strait (JEMS), 1999. Standard Operating Procedure for CTD processing of JEMS data, Friday Harbor Laboratories, University of Washington.

Kudela, M.R, et al. 2008. "New Insights into the Controls and Mechanisms of Plankton Productivity in Coastal Upwelling Waters of the Northern California Current System." *The Oceanography Society* 21.4: 1-14.

Lorenzen, C. J, and Downs, J. N. 1986. The specific absorption coefficients of chlorophyllide a and pheophorbide a in 90% acetone, and comments on the fluorometric determination of chlorophyll and pheopigments. *Limnology Oceanography,31*(2): 449-452.

Mann, K.H. and Lazier, J.R.N.. 1991. Dynamics of marine ecosystems: biological-physical interactions in the oceans. Blackwell Scientific Publications Inc.: 111-287.

McLaughlin, R. 2009. Inter-annual variation in temperature, salinity, and dissolved oxygen in San Juan Channel: patterns and external driving forces. University of Washington, Friday Harbor Labs: 1-28.

Meyer, B. 2011. Factors influencing phytoplankton and dissolved oxygen in San Juan Channel: a spatial and temporal assessment. University of Washington, Friday Harbor Labs: 1-22.

Multivariate ENSO Index. 2012. *Earth System Research Laboratory: Physical Sciences Division*. NOAA.

Newton, J.A., et al. 2002. Seasonal patterns and controlling factors of primary production in Puget Sound's Central Basin and Possession Sound. *Washington Department of Ecology Report, 02-03-059.*

Tide Data: Friday Harbor, WA. 2012.*Tides & Currents*. NOAA. <http://tidesandcurrents.noaa.gov/data_menu.shtml?stn=9449880%20Friday%20Harbor,%20WA&type=Tide%20Data>.

Thomas, K. 2011. Seasonal and tidal effects on water density gradients in the San Juan Channel. University of Washington, Friday Harbor Labs: 1-44.

Environment Canada. Water Survey. Real-time hydrometric data. October 2012. <http://www.ec.gc.ca/eau-water/default.asp?lang=En&n=45BBB7B8-1

Winkler, L.S. 1888. The determination of dissolved oxygen. Ber. Dtsche. Chem. Ges. 21: 2843-2855.

Figure 1: Station locations and names: North Station (48˚35.00' N 123˚02.50' W) and South Station (48˚25.20' N, 122˚56.60' W).

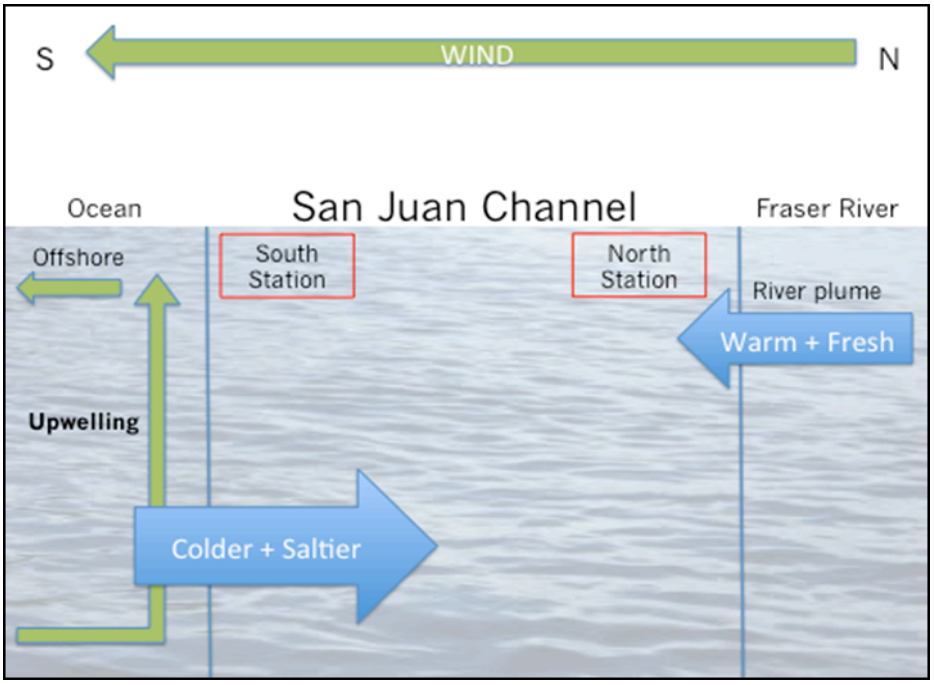

Figure 2: Conceptual model of external factors: oceanic (upwelling) and Fraser River at N and S during spring and summer.

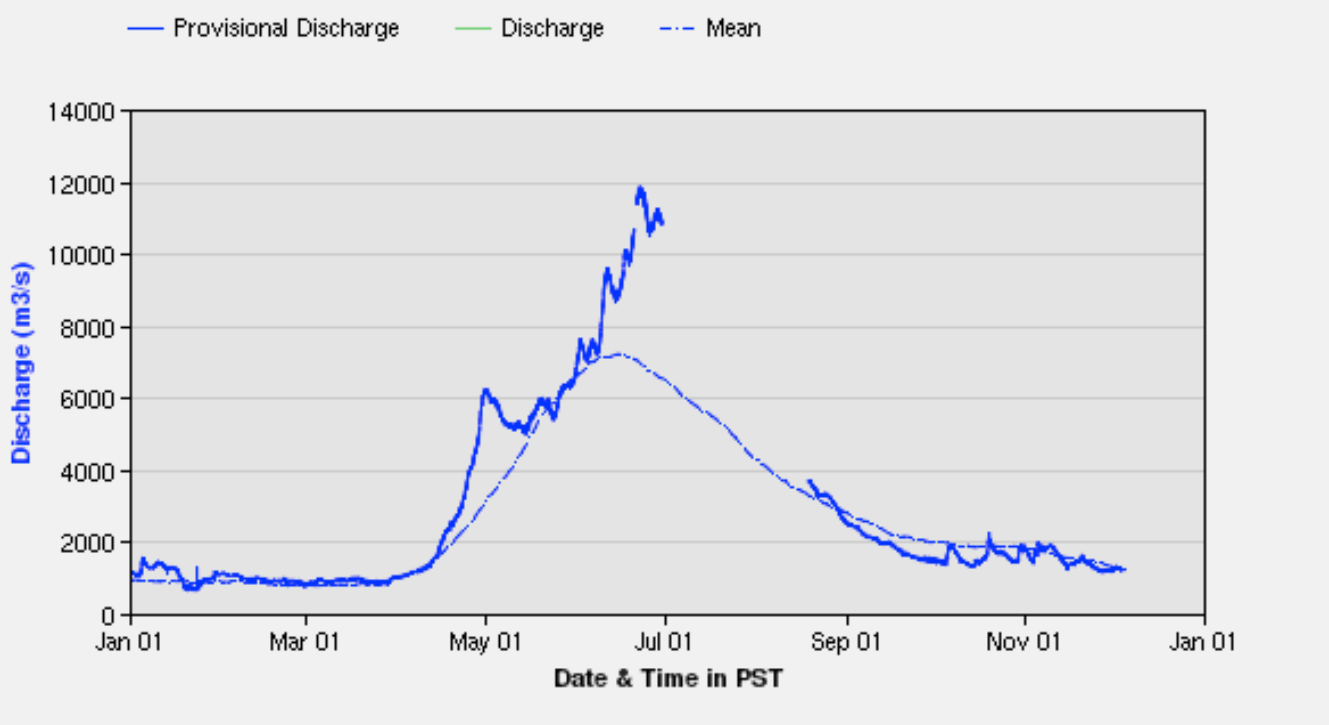

Figure 3: Fraser River discharge January 2012-January 2013 (historical average and 2012 provisional values).

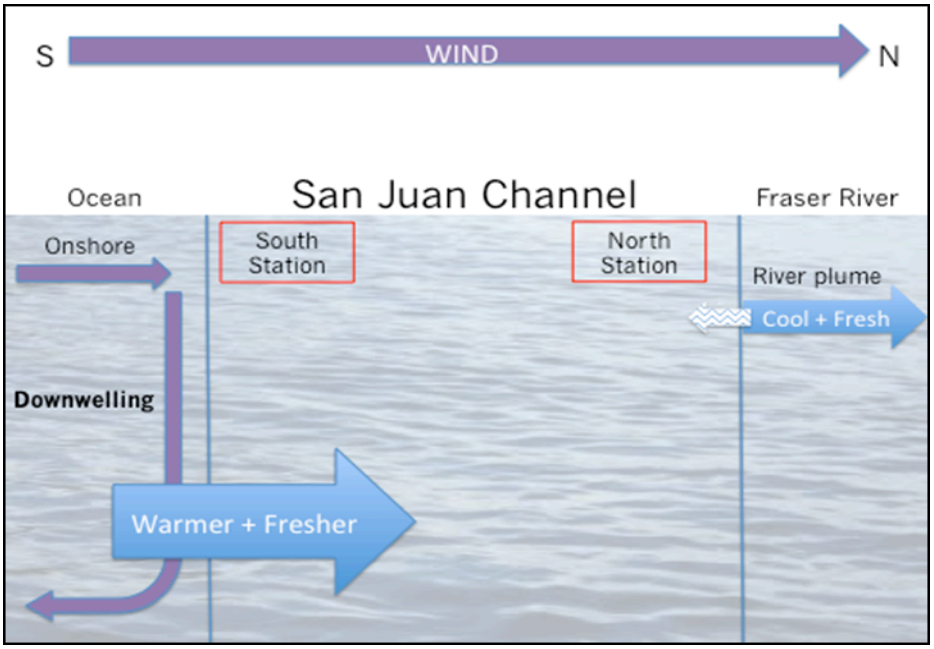

Figure 4: Conceptual model of external factors: oceanic (downwelling) and Fraser River at N and S during fall and winter.

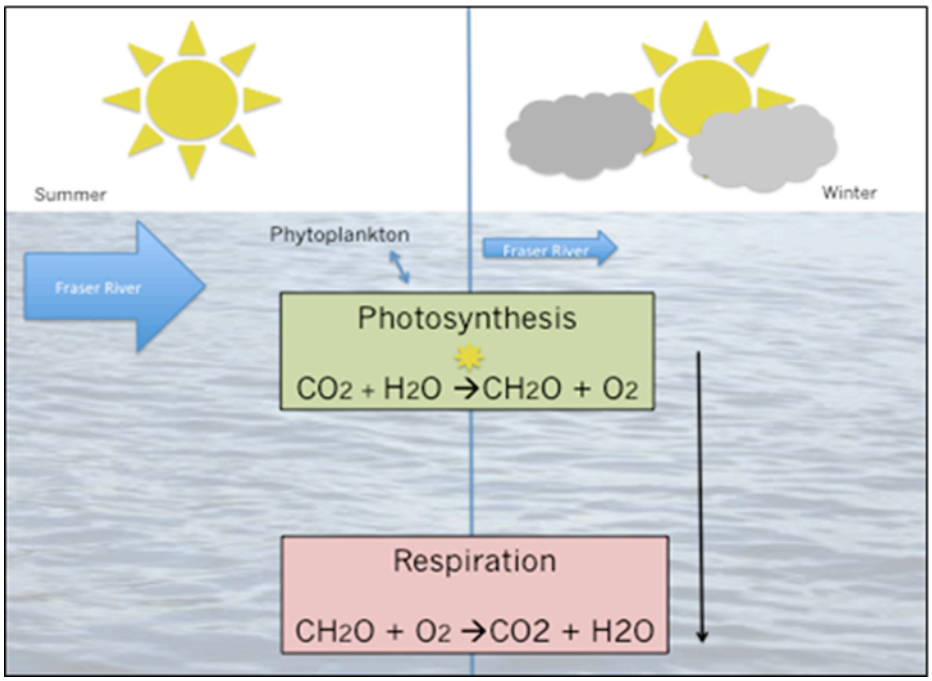

Figure 5: Conceptual model of photosynthesis and respiration (biological processes of focus) in the water column. Summer is associated with more sunlight and higher Fraser River discharge, and winter is associated with less sunlight and less Fraser River discharge. Photosynthesis typically occurs at surface. Respiration occurs all throughout water column.

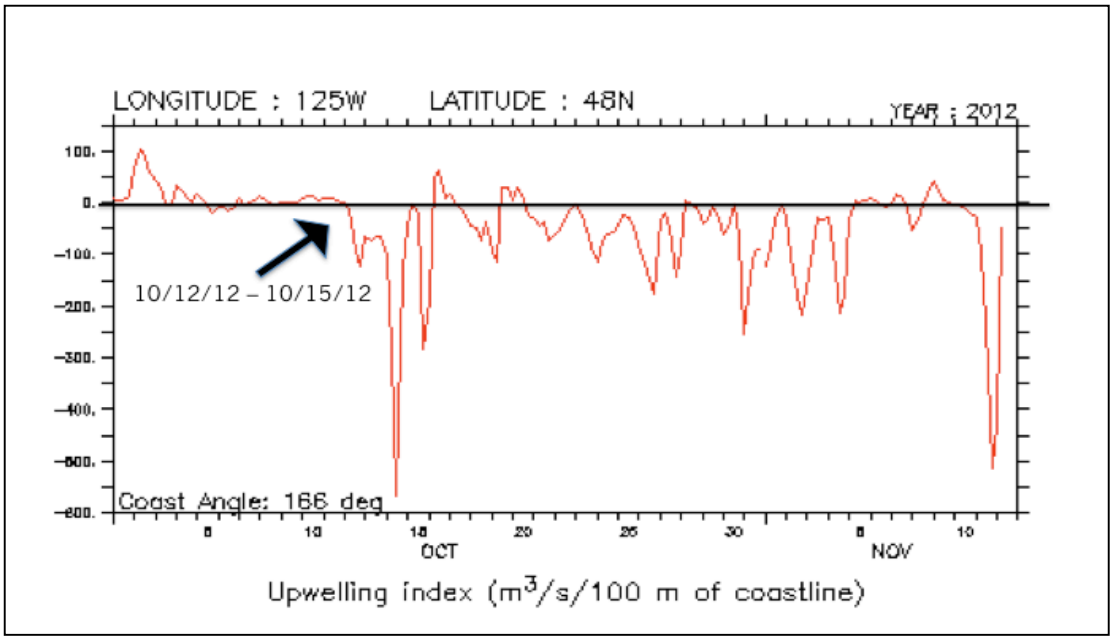

Figure 6: NOAA fall 2012 upwelling index. Values predominantly above line are indicative of upwelling. Values predominantly below the line are indicative of downwelling.

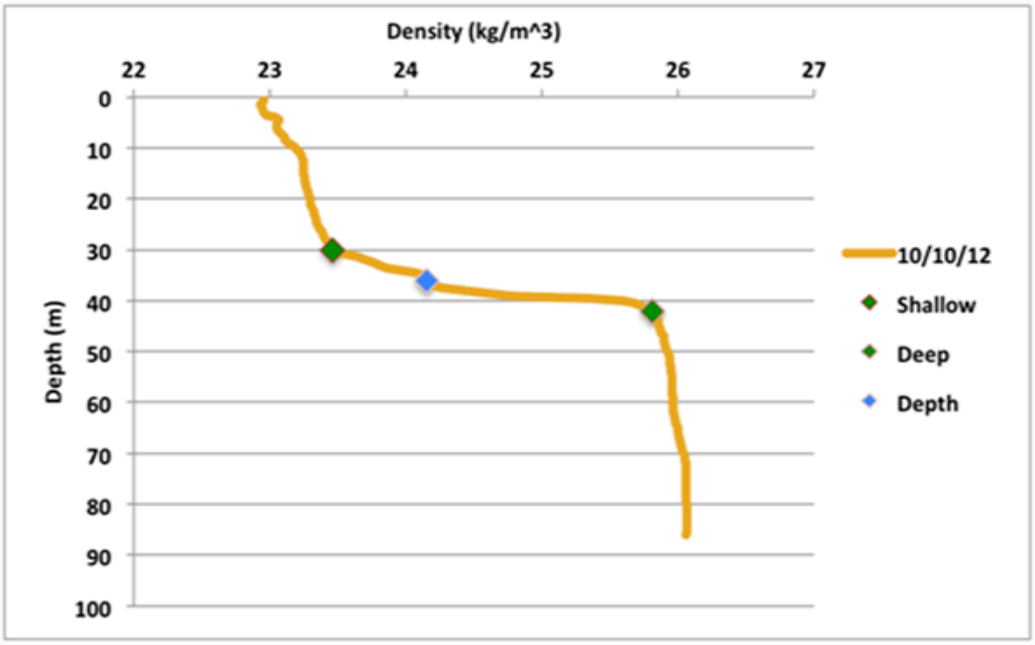

Figure 7: Pycnocline width and depth at South station 10/10/2012.

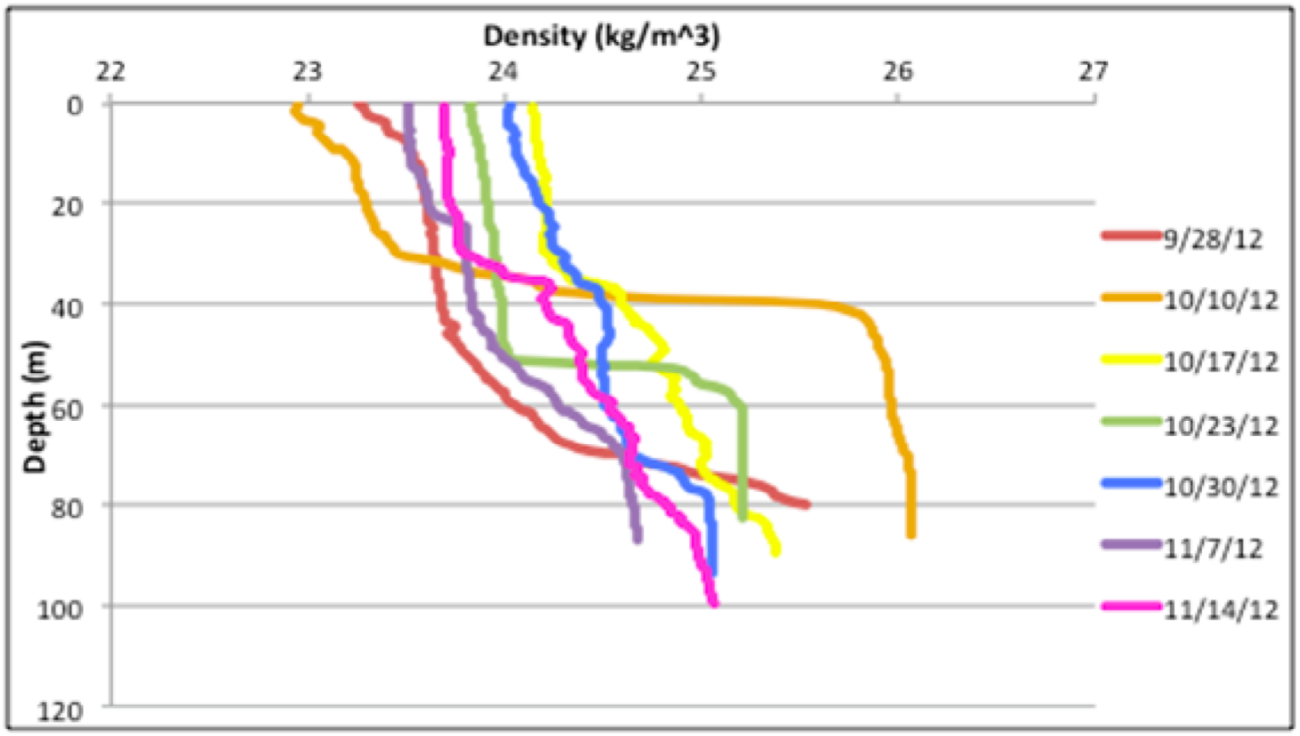

Figure 8: South station density versus depth fall 2012.

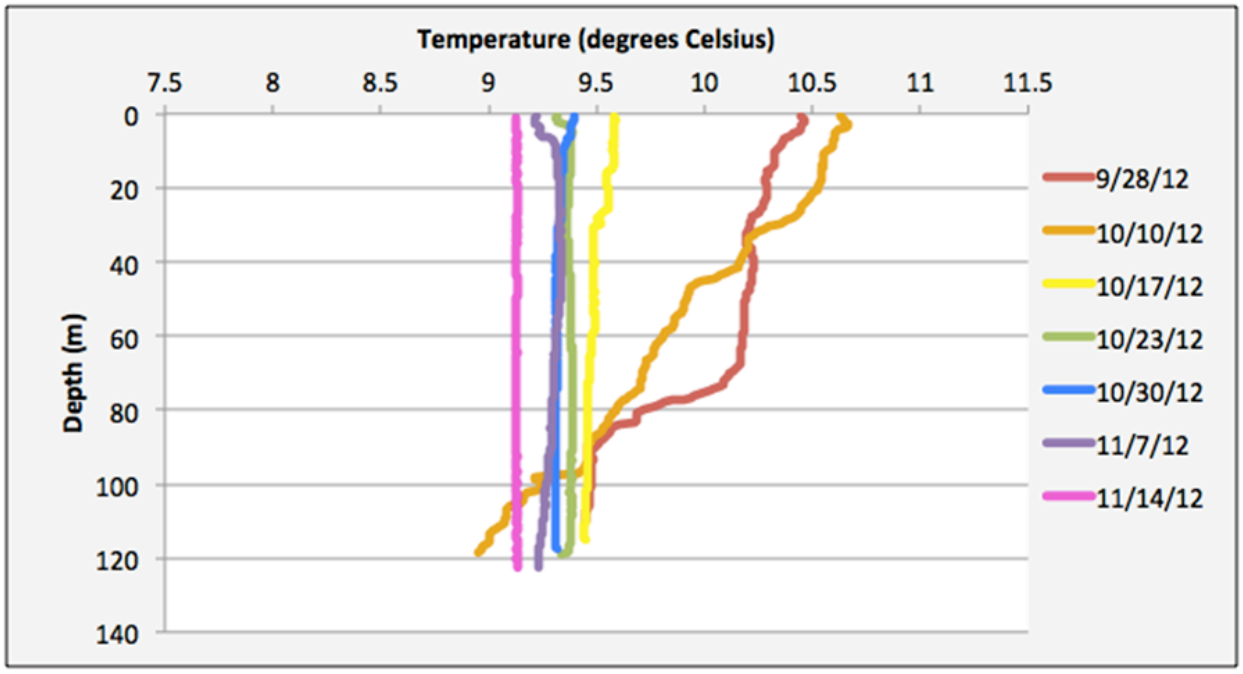

Figure 9: North station temperature versus depth fall 2012.

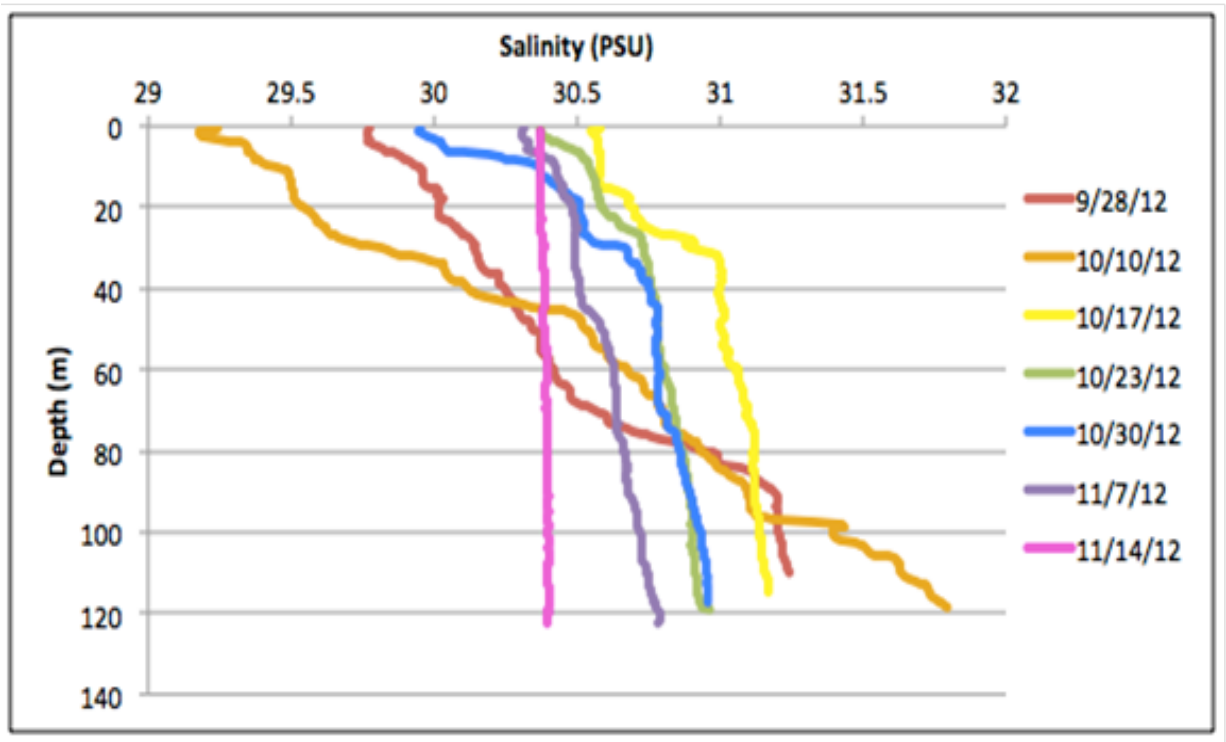

Figure 10: North station salinity versus depth fall 2012.

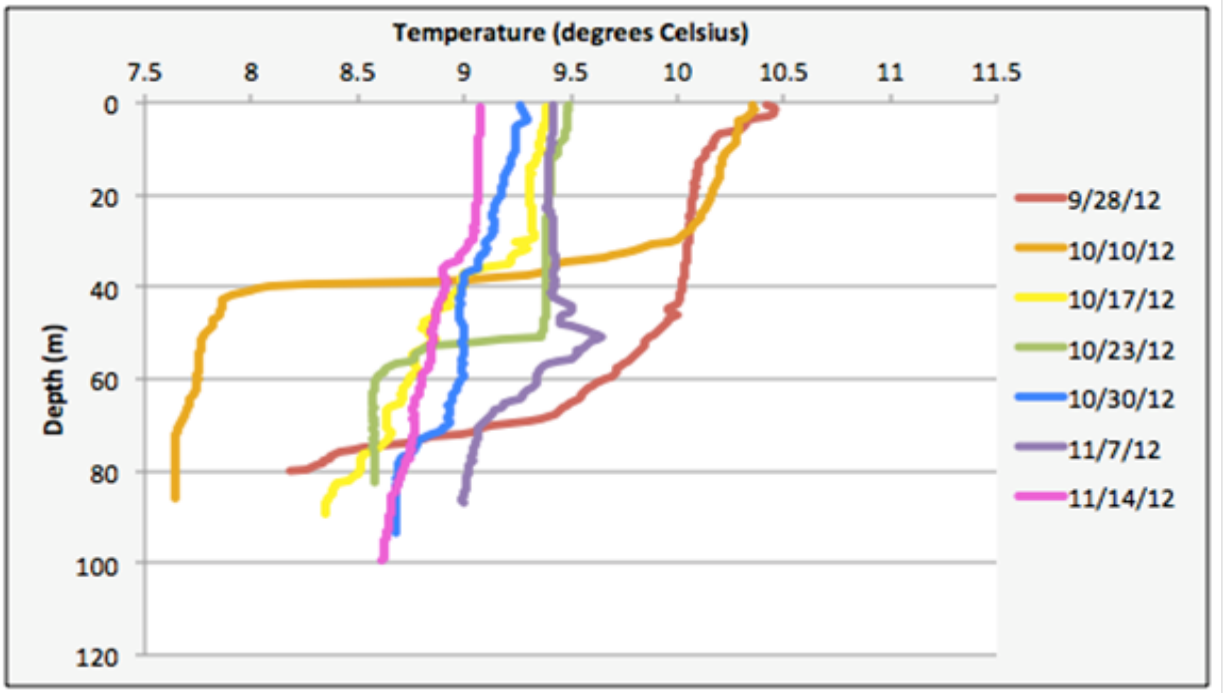

Figure 11: South station temperature versus depth fall 2012.

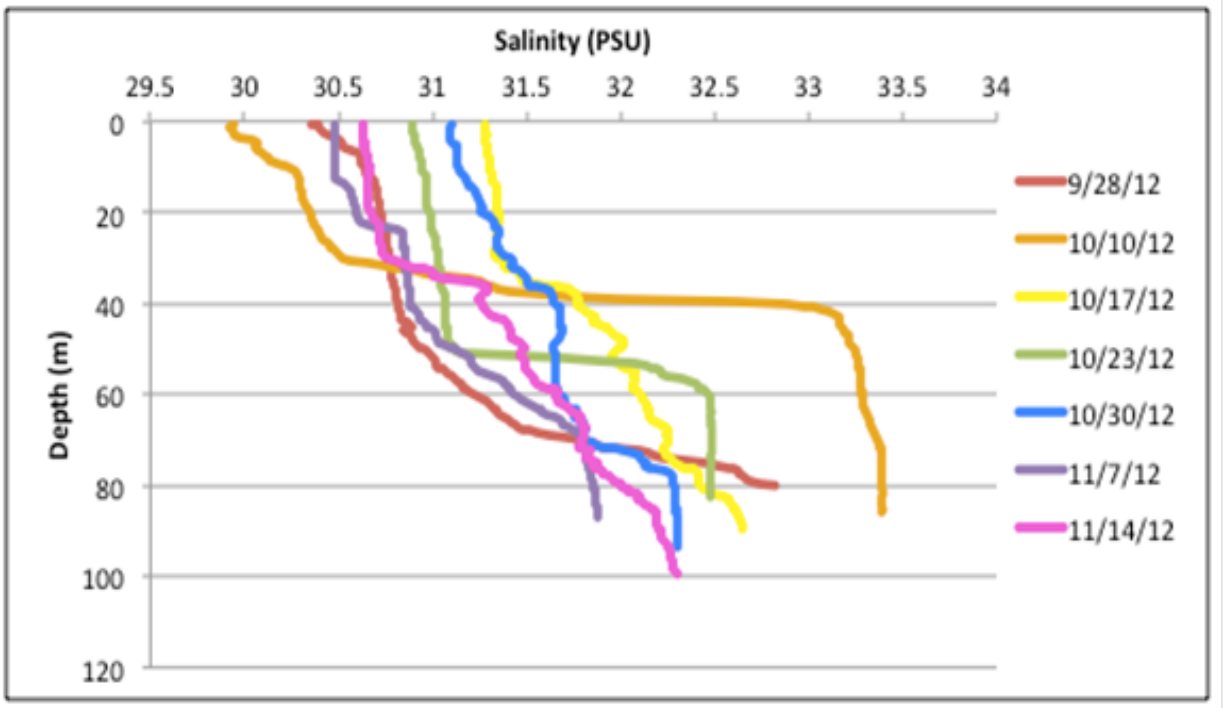

Figure 12: South station salinity versus depth fall 2012.

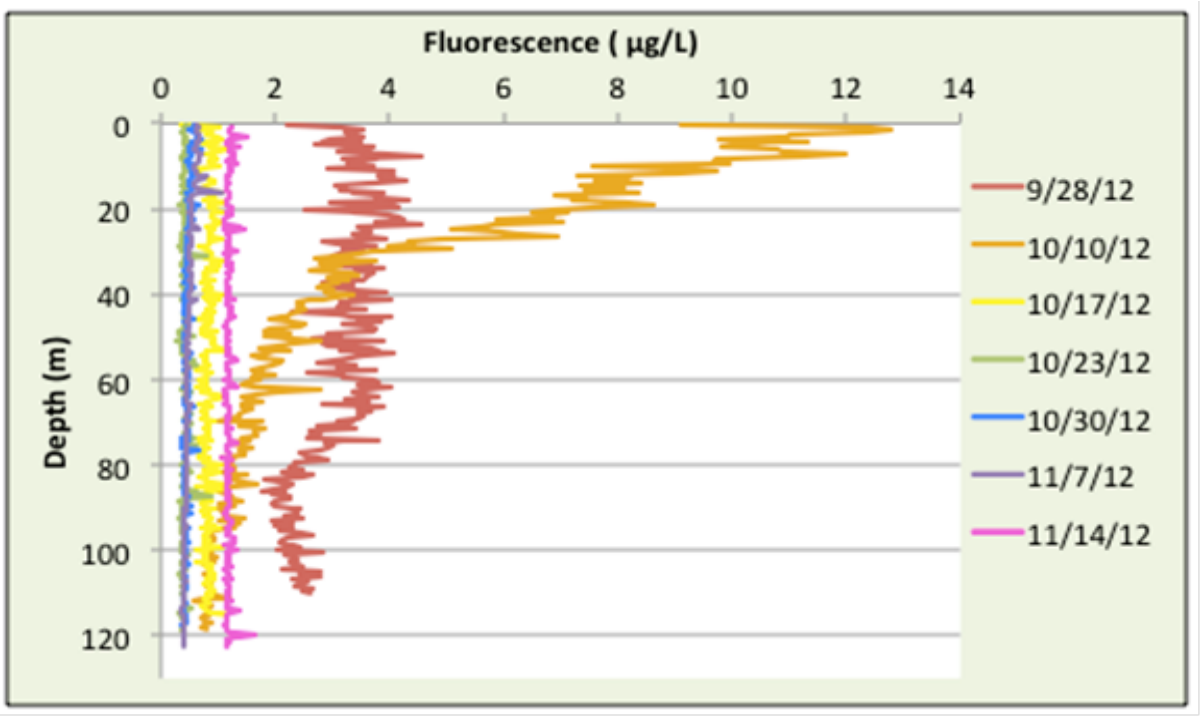

Figure 13: North station chlorophyll fluorescence fall 2012.

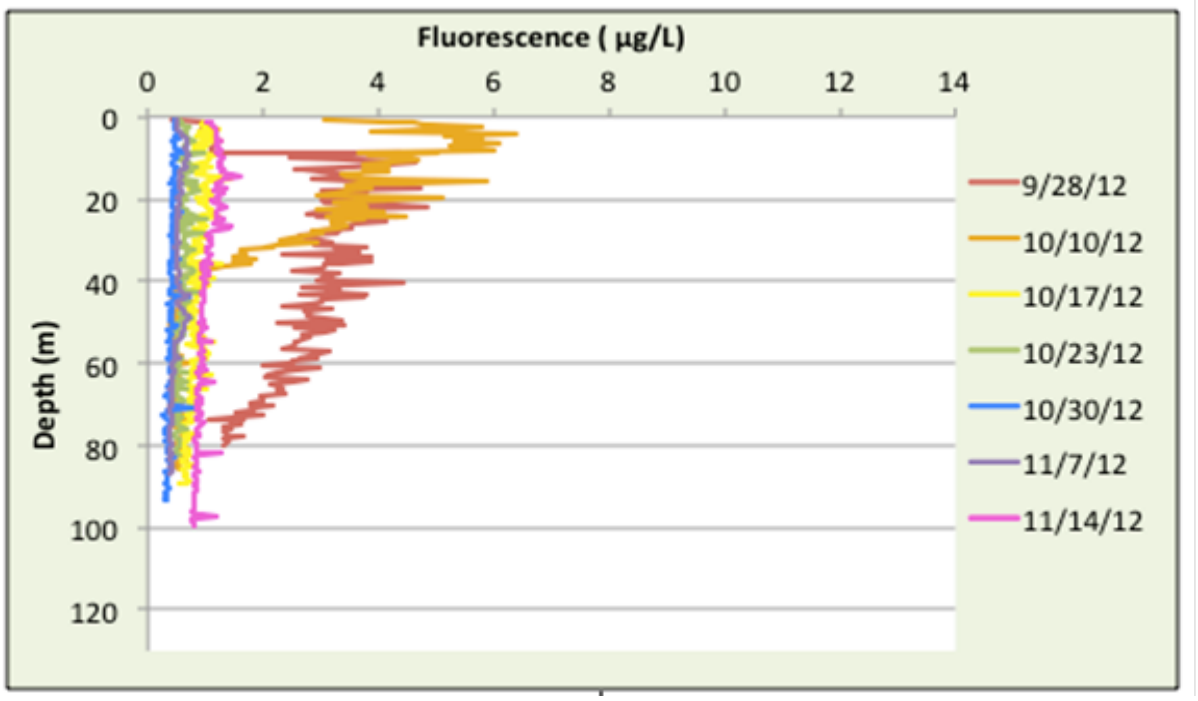

Figure 14: South station chlorophyll fluorescence versus depth fall 2012.

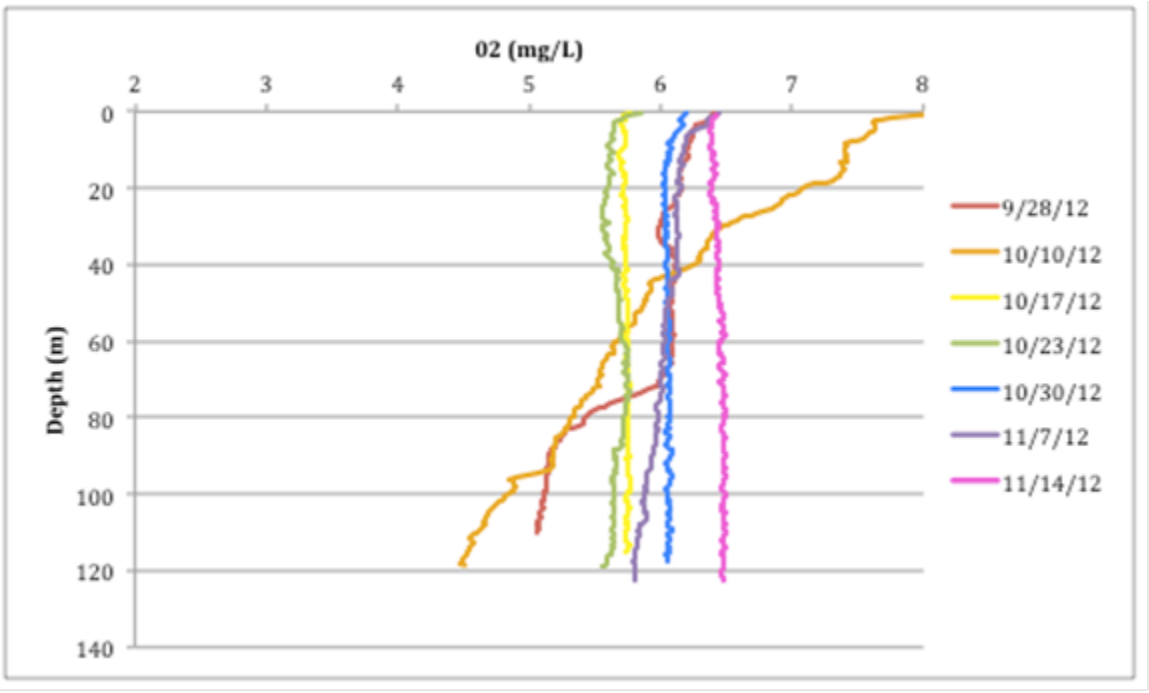

Figure 15: North station dissolved oxygen concentrations fall 2012.

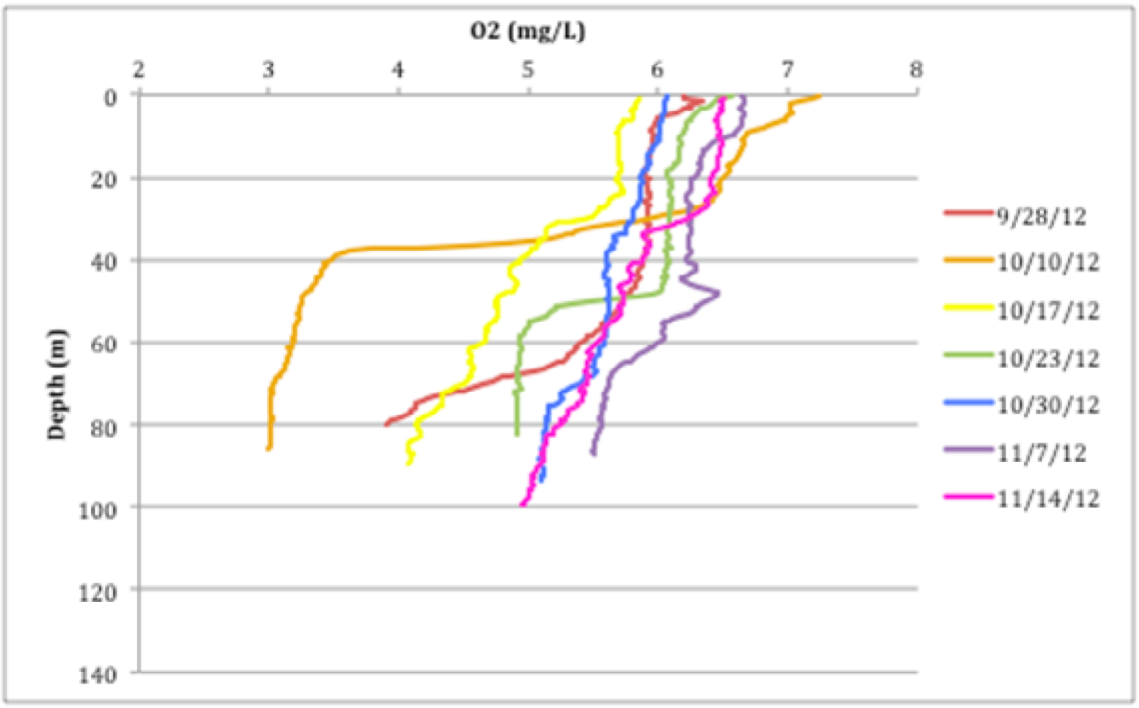

Figure 16: South station dissolved oxygen versus depth fall 2012.

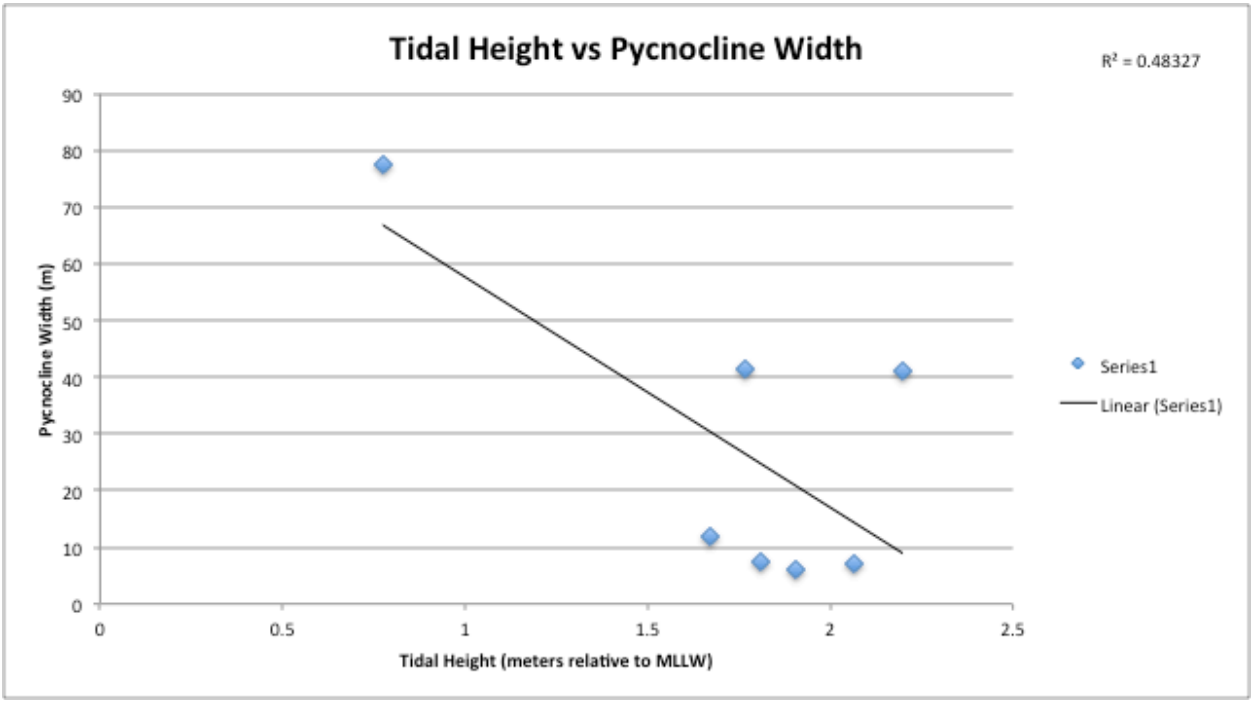

Figure 17: Tidal height versus pycnocline width during fall 2012.

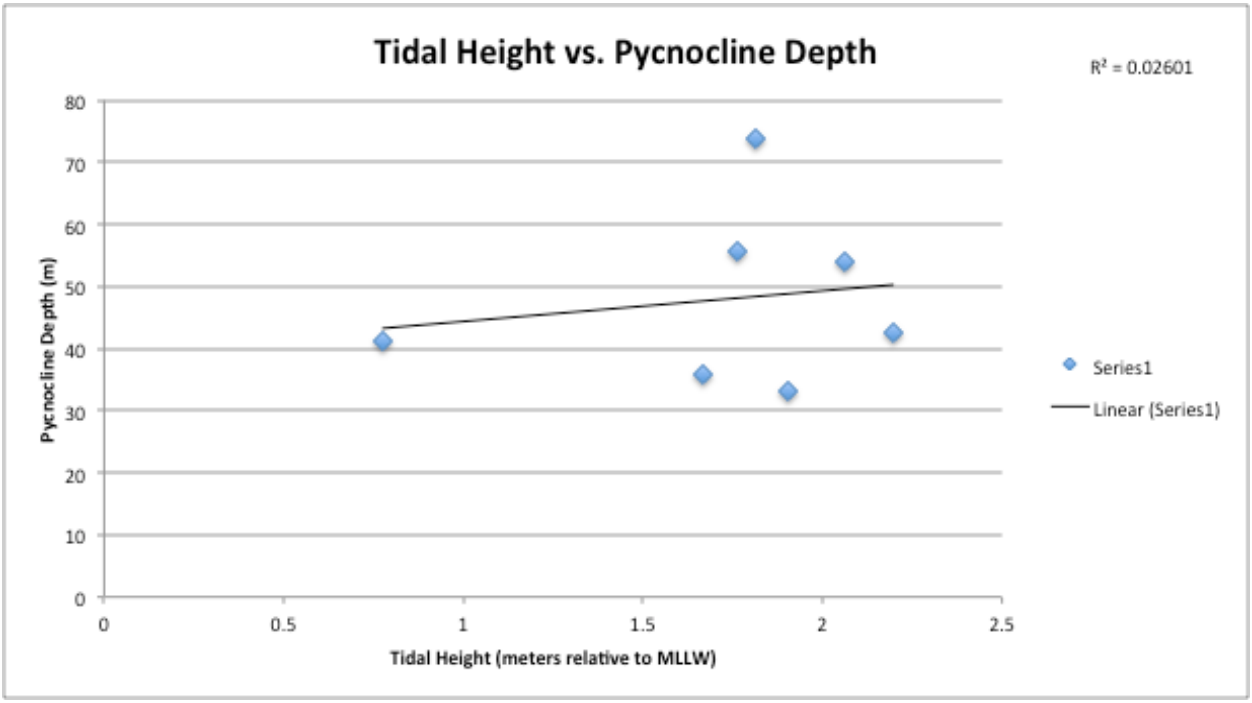

Figure 18: Tidal height versus pycnocline depth during fall 2012.

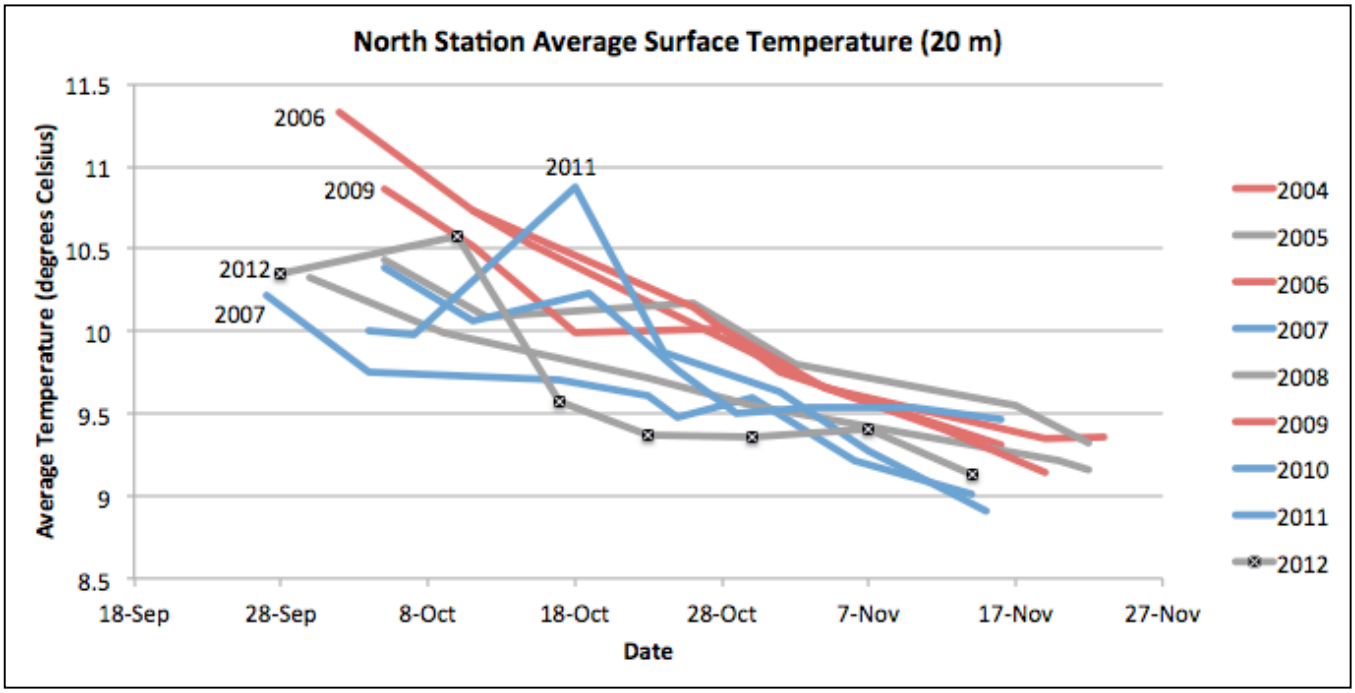

Figure 19: North station interannual surface (0-20m) temperature (2004-2012). Plots are color-coded based on ENSO index: red=El Niño; grey=neutral; blue=La Niña.

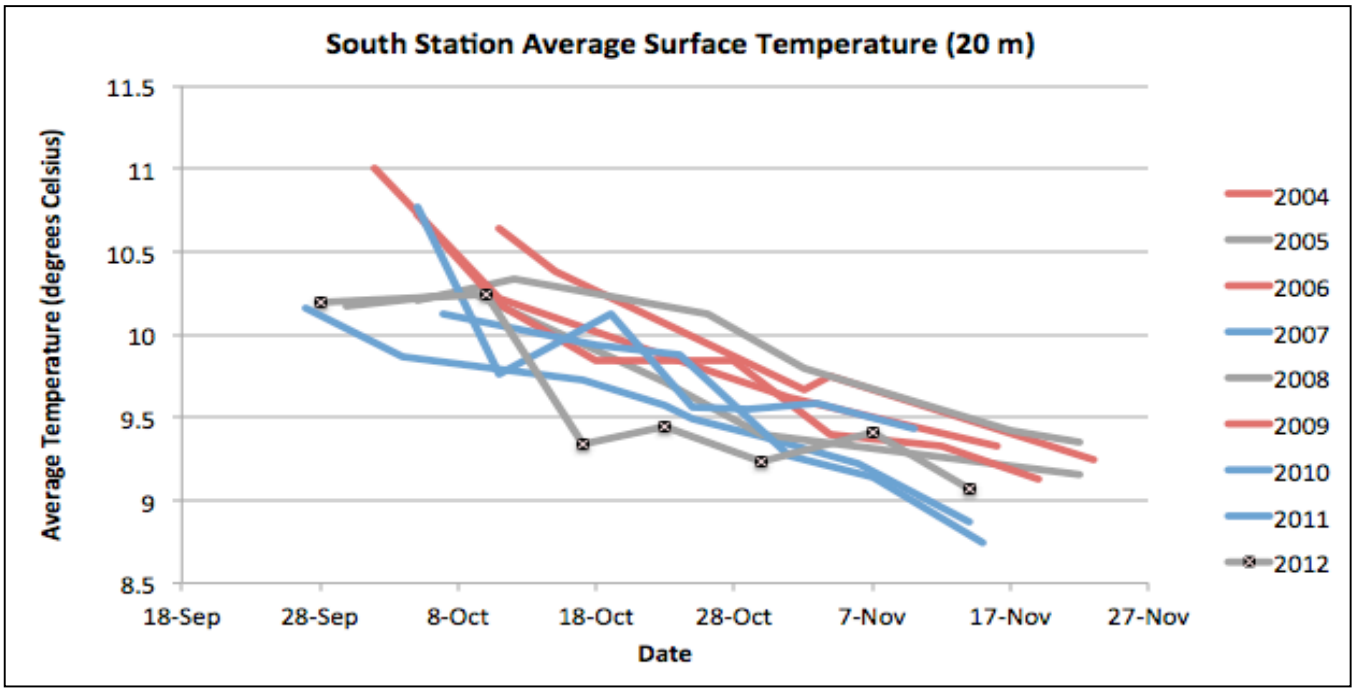

Figure 20: South station interannual surface (0-20m) temperature (2004-2012). Plots are color-coded based on ENSO index: red=El Niño; grey=neutral; blue=La Niña.

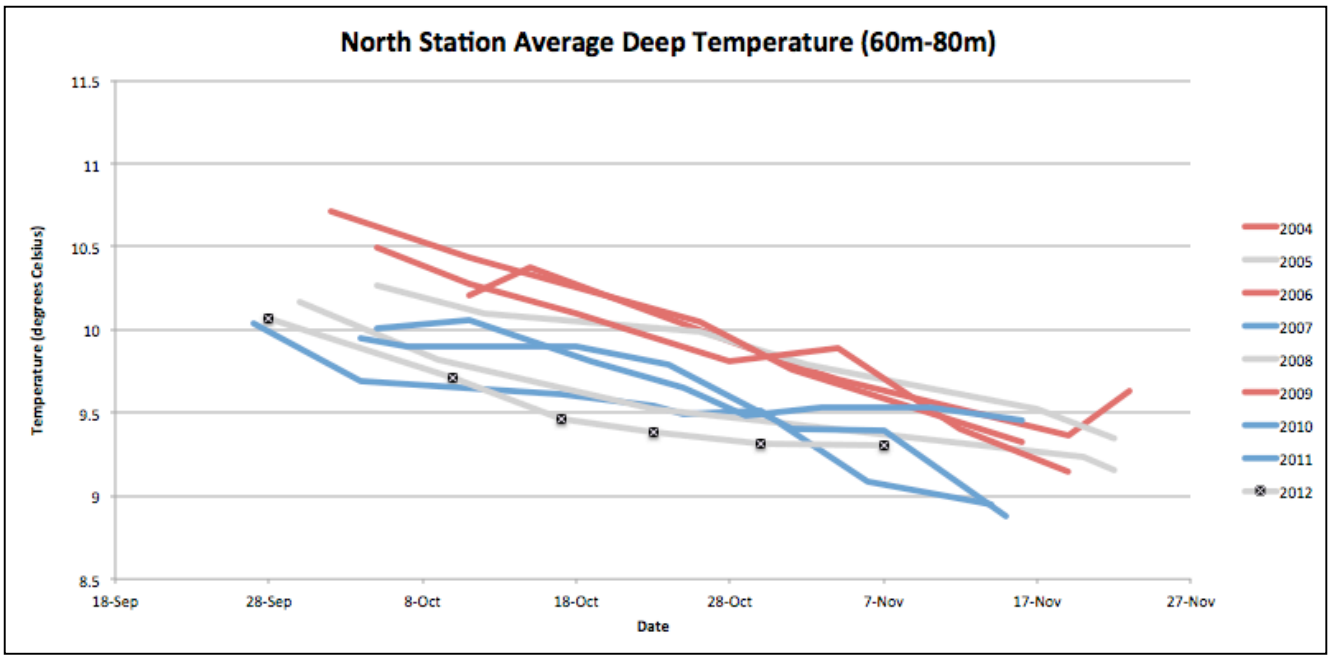

Figure 21: North station interannual deep (60-80m or bottom [whichever comes first]) temperature (2004-2012). Plots are color-coded based on ENSO index: red=El Niño; grey=neutral; blue=La Niña.

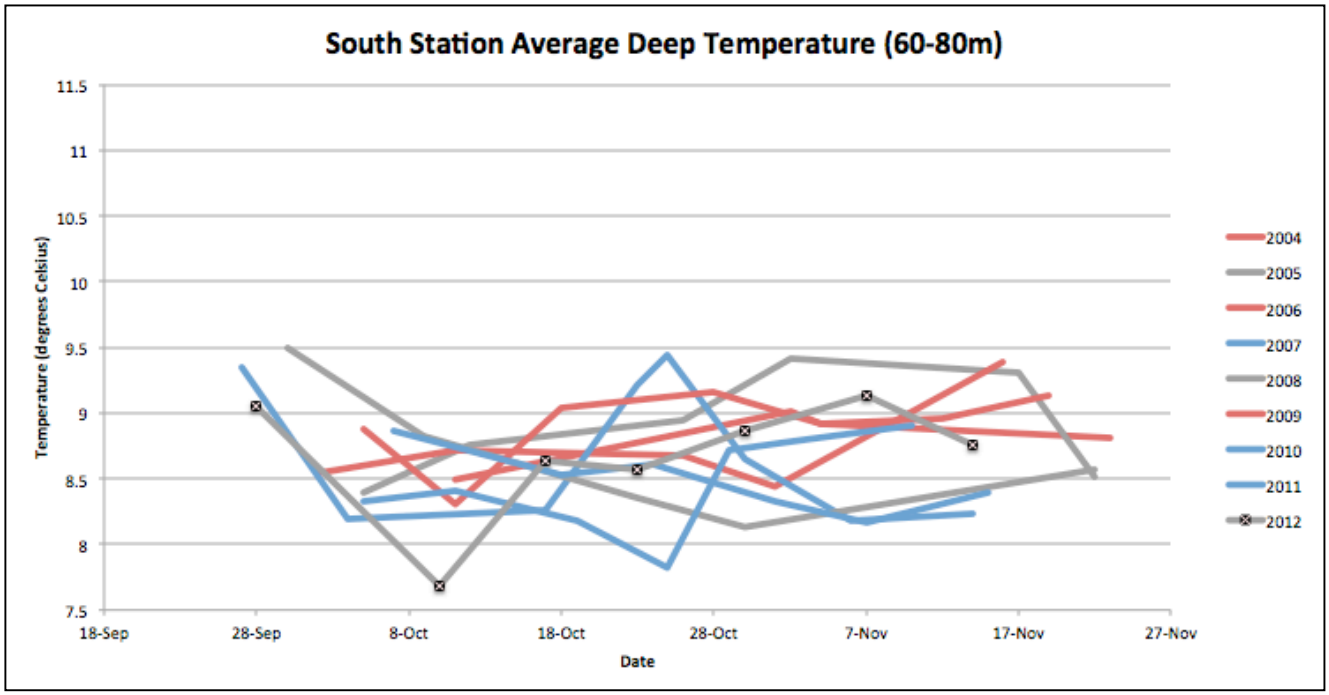

Figure 22: South station interannual deep (60-80m or bottom [whichever comes first]) temperature (2004-2012). Plots are color-coded based on ENSO index: red=El Niño; grey=neutral; blue=La Niña.

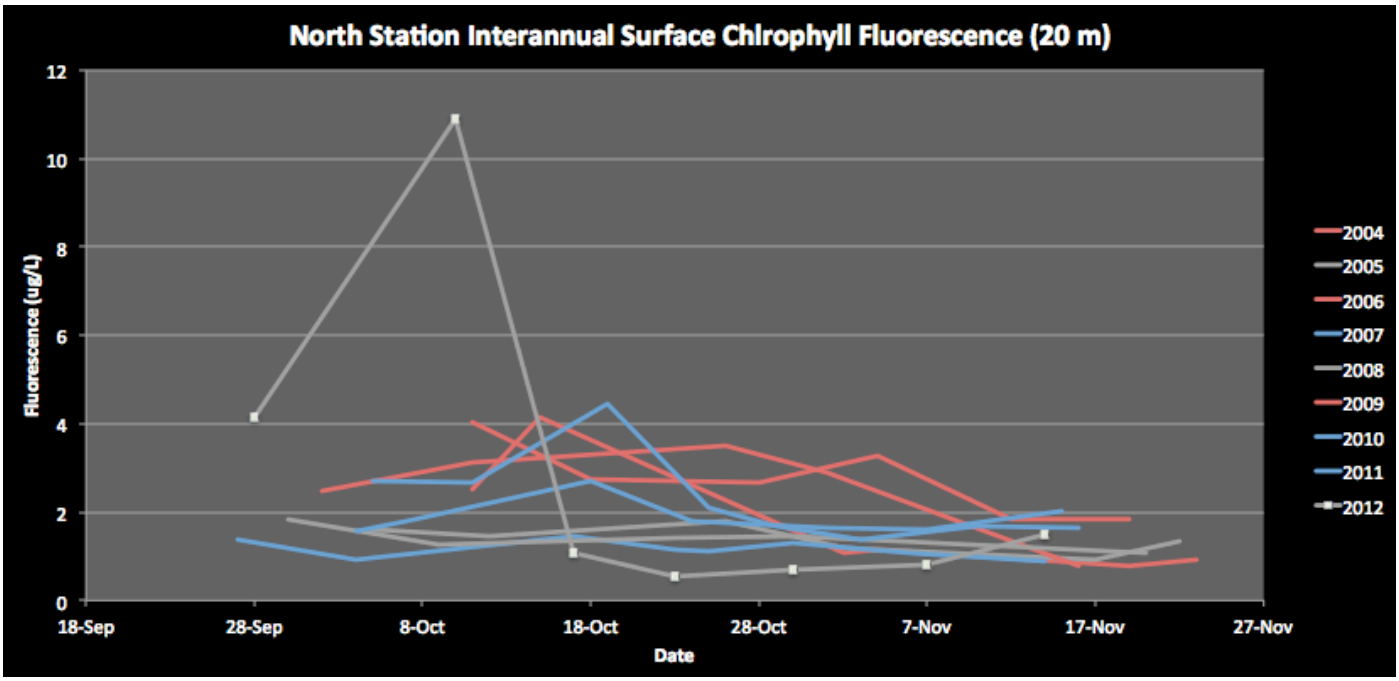

Figure 23: North station interannual surface (0-20m) chlorophyll fluorescence (2004-2012). Plots are color-coded based on ENSO index: red=El Niño; grey=neutral; blue=La Niña.

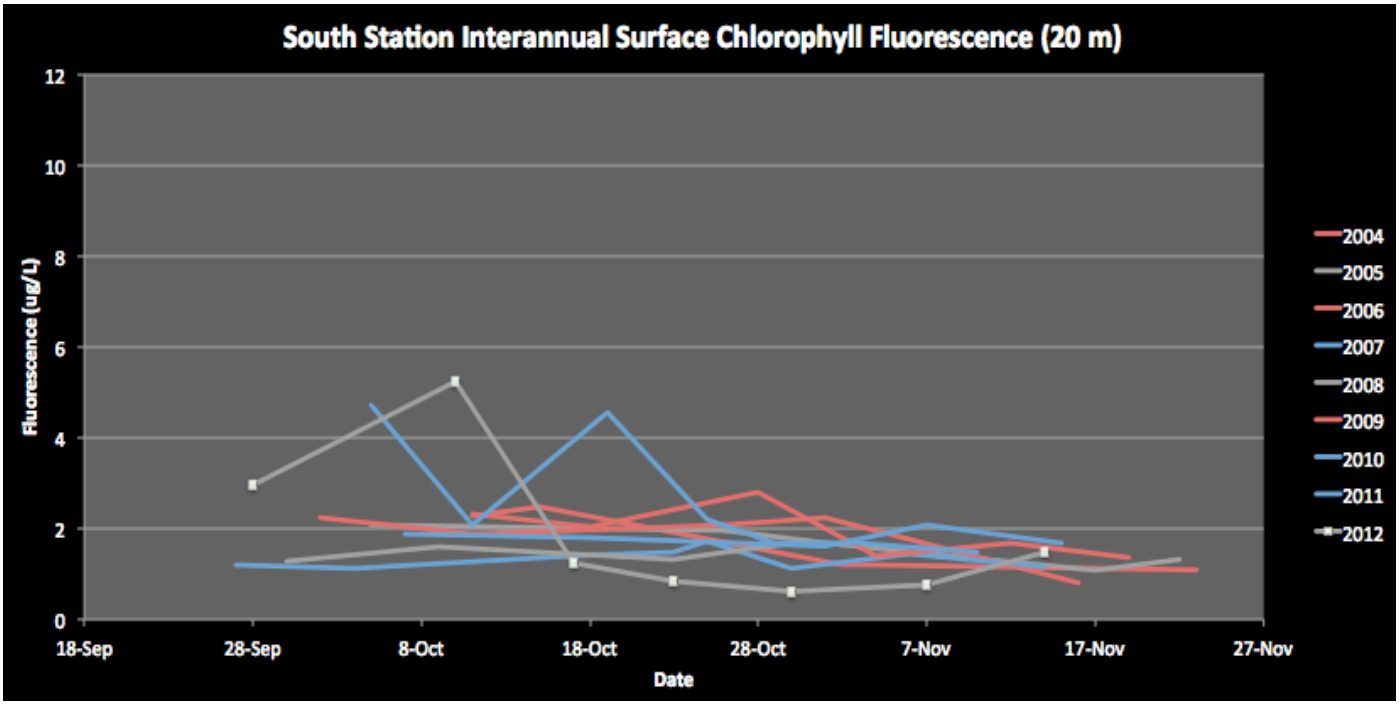

Figure 24: South Station interannual surface (0-20m) chlorophyll fluorescence (2004-2012). Plots are color-coded based on ENSO index: red=El Niño; grey=neutral; blue=La Niña.

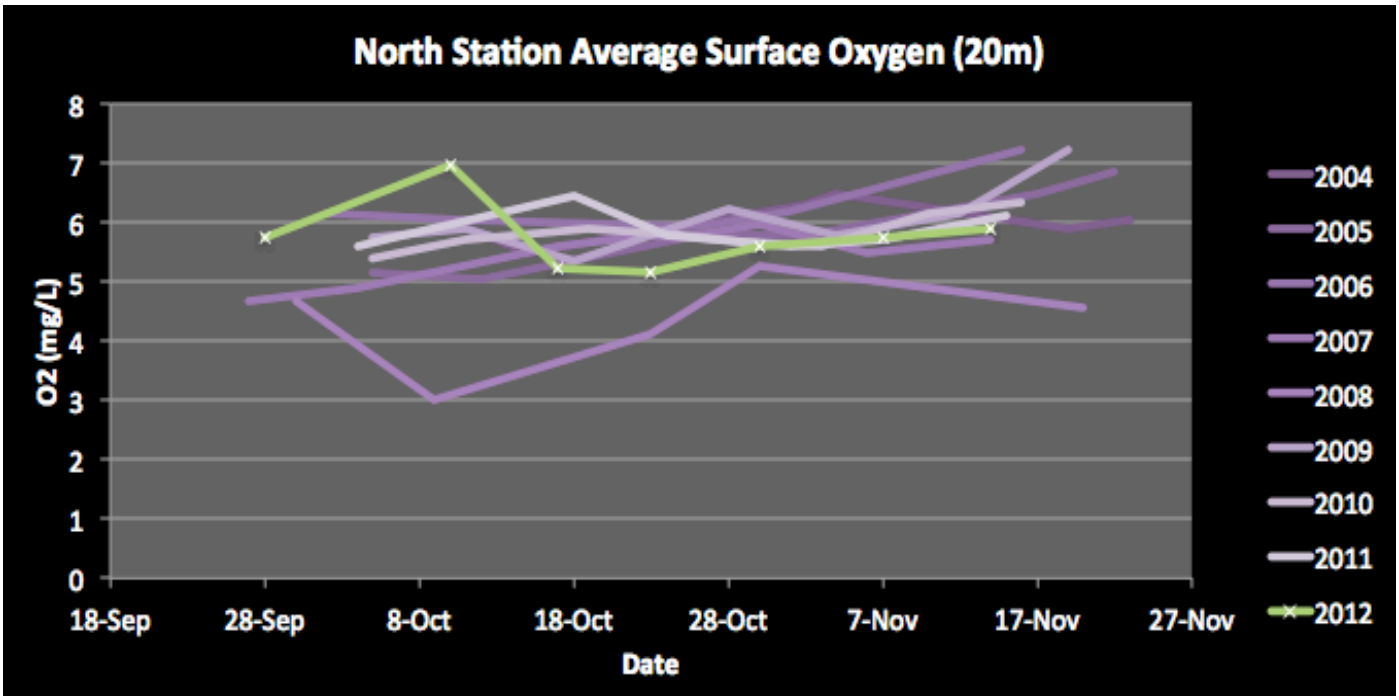

Figure 25: North station interannual surface (0-20m) dissolved oxygen (2004-2012). Purple plots get lighter as time progresses; green plot is 2012.

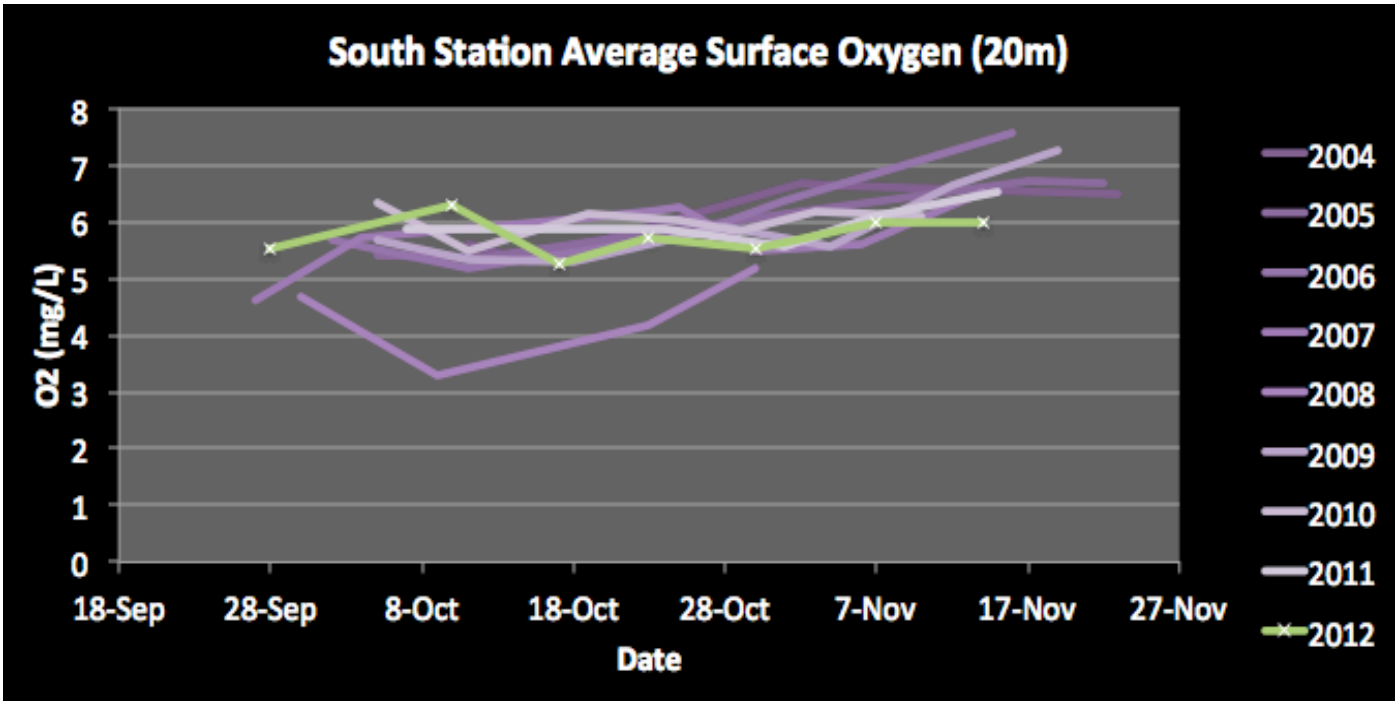

Figure 26: South station interannual surface (0-20m) dissolved oxygen (2004-2012). Purple plots get lighter as time progresses; green plot is 2012.

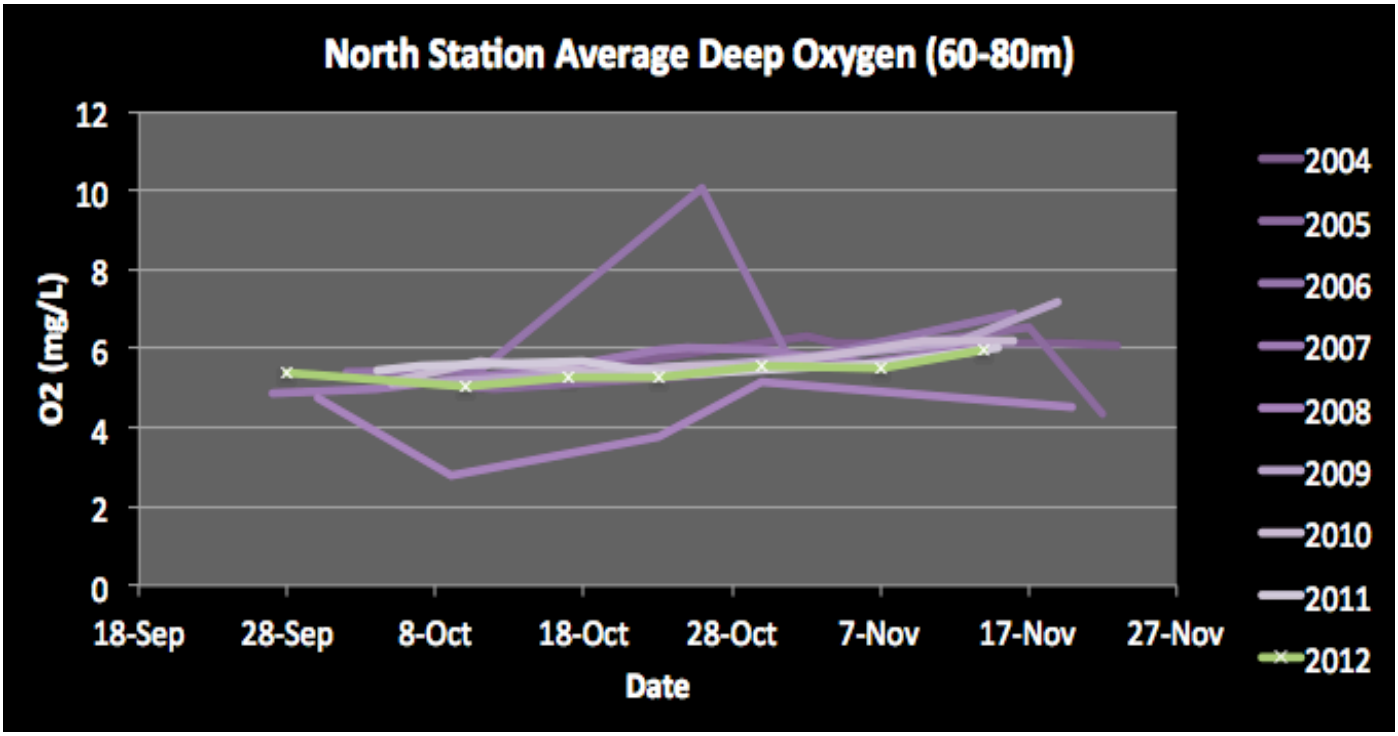

Figure 27: North station interannual deep (60-80m or bottom [whichever comes first]) dissolved oxygen (2004-2012). Purple plots get lighter as time progresses; green plot is 2012.

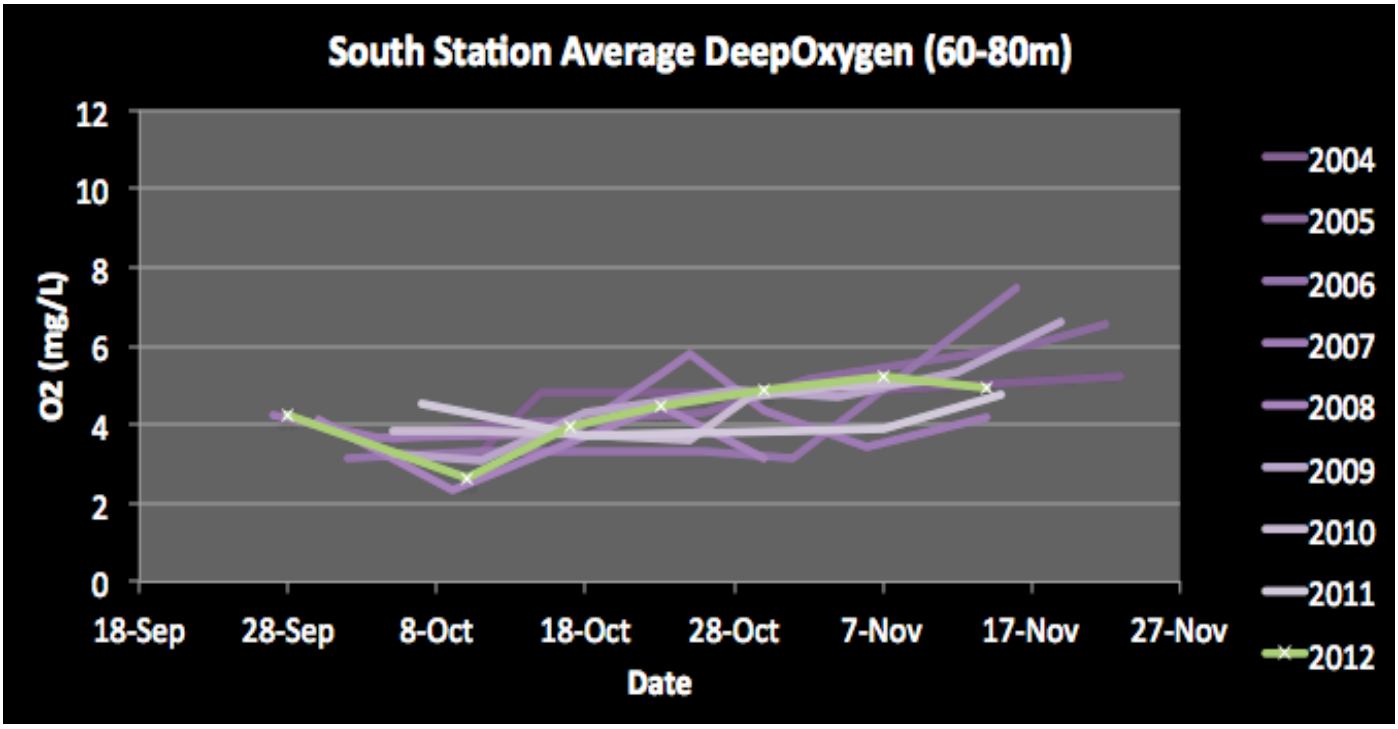

Figure 28: South station interannual deep (60-80m or bottom [whichever comes first]) dissolved oxygen (2004-2012). Purple plots get lighter as time progresses; green plot is 2012.

Table 1: Cruise dates fall 2012.

Cruise Number	Cruise Date
1	9/28/2012
2	10/10/2012
3	10/17/2012
4	10/23/2012
5	10/30/2012
6	11/7/2012
7	11/14/2012

Table 2: Tidal height and direction at south station during 2012 cruises.

Cruise	Tidal Height (MLLW)	Ebb/Flood
1	0.774m	Flood
2	1.67m	Flood
3	1.766m	Ebb
4	2.064m	Flood
5	1.812m	Ebb
6	2.1985m	Flood
7	1.906m	Ebb

Table 3: Correlation coefficient values (R^2) for chlorophyll versus density.

Date	Station	R^2=
9/28/2012	N	0.59
9/28/2012	S	0.17
10/10/2012	N	0.76
10/10/2012	S	0.84
10/17/2012	N	0.03
10/17/2012	S	0.45
10/23/2012	N	0.00
10/23/2012	S	0.32
10/30/2012	N	0.52
10/30/2012	S	0.36
11/7/2012	N	0.69
11/7/2012	S	0.65
11/14/2012	N	0.02
11/14/2012	S	0.75

Table 4: Correlation coefficient values (R^2) for chlorophyll versus dissolved oxygen.

Date	Station	R^2=
9/28/2012	N	0.62
9/28/2012	S	0.19
10/10/2012	N	0.85
10/10/2012	S	0.90
10/17/2012	N	0.01
10/17/2012	S	0.47
10/23/2012	N	0.05
10/23/2012	S	0.33
10/30/2012	N	0.14
10/30/2012	S	0.35
11/7/2012	N	0.62
11/7/2012	S	0.74
11/14/2012	N	0.02
11/14/2012	S	0.77

Table 5: Correlation coefficient values (R^2) for density versus dissolved oxygen.

Date	Station	R^2=
9/28/2012	N	0.93
9/28/2012	S	0.98
10/10/2012	N	0.98
10/10/2012	S	0.97
10/17/2012	N	0.53
10/17/2012	S	0.96
10/23/2012	N	0.06
10/23/2012	S	0.95
10/30/2012	N	0.22
10/30/2012	S	0.99
11/7/2012	N	0.96
11/7/2012	S	0.92
11/14/2012	N	0.85
11/14/2012	S	0.99